



Search for a right-handed gauge boson decaying into a high-momentum heavy neutrino and a charged lepton in pp collisions with the ATLAS detector at $\sqrt{s} = 13$ TeV

The ATLAS Collaboration ^{*}

ARTICLE INFO

Article history:

Received 30 April 2019

Received in revised form 4 August 2019

Accepted 22 August 2019

Available online 18 September 2019

Editor: M. Doser

ABSTRACT

A search for a right-handed gauge boson W_R , decaying into a boosted right-handed heavy neutrino N_R , in the framework of Left-Right Symmetric Models is presented. It is based on data from proton–proton collisions with a centre-of-mass energy of 13 TeV collected by the ATLAS detector at the Large Hadron Collider during the years 2015, 2016 and 2017, corresponding to an integrated luminosity of 80 fb^{-1} . The search is performed separately for electrons and muons in the final state. A distinguishing feature of the search is the use of large-radius jets containing electrons. Selections based on the signal topology result in smaller background compared to the expected signal. No significant deviation from the Standard Model prediction is observed and lower limits are set in the W_R and N_R mass plane. Mass values of the W_R smaller than 3.8–5 TeV are excluded for N_R in the mass range 0.1–1.8 TeV.

© 2019 The Author. Published by Elsevier B.V. This is an open access article under the CC BY license (<http://creativecommons.org/licenses/by/4.0/>). Funded by SCOAP³.

1. Introduction

Over the past decades, there have been several important developments at the theoretical and experimental frontiers to address the question of neutrino mass generation, which is not explained in the Standard Model (SM) of particle interactions. A widely adopted approach to explain small neutrino masses is the so-called seesaw mechanism [1], where the light neutrinos acquire their Majorana masses from dimension-5 operators through electroweak symmetry breaking. The simplest seesaw mechanism can be categorised into a few different classes, such as the Type-I [2–4], Type-II [5–7] and Type-III [5,8] seesaw scenarios. Type-I and Type-II models can further be embedded into a Left-Right Symmetric Model (LRSM) [9–11]. The LRSM contains SM-singlet heavy neutrinos N_R , which are introduced as the parity gauge partners of the corresponding left-handed neutrino fields, and a right-handed gauge boson W_R .

The LRSM framework provides a natural set-up for the seesaw mechanism and offers several features including parity symmetry at high energy, mass generation of the light and heavy neutrinos, explanation of parity violation in the SM and existence of the right-handed charged current. This model can naturally explain the small neutrino masses through the Type-I seesaw via the right-handed neutrinos, and the Type-II seesaw via SU(2)-triplet scalars. Both the Type-I and Type-II contributions can coexist. In the LRSM,

left-handed neutrinos (SM neutrinos) as well as the right-handed neutrinos are considered to be Majorana particles (i.e. to be their own antiparticles). The LRSM thus features violation of the global lepton number symmetry of the SM. Hence, the model can be tested by observing lepton-number-violating processes, such as the Keung–Senjanović process [12], shown in Fig. 1.

Searches by the ATLAS [13,14] and CMS [15–19] collaborations for signatures of LRSMs have considered the final state containing two charged leptons and two jets and have excluded regions of the (m_{W_R}, m_{N_R}) parameter space for m_{W_R} and m_{N_R} up to several TeV, where m_{N_R} and m_{W_R} denote the masses of N_R and W_R , respectively.

This search is focused on the regime where the W_R is very heavy compared with the N_R ($m_{N_R}/m_{W_R} \leq 0.1$), and investigates an alternative signature for $W_R \rightarrow N_R \ell$ decays, following Ref. [20]. The probed mass regime enables exploration of a parameter space complementary to the one used in previous searches that reconstruct the N_R decay into a charged lepton and two jets, later referred to as the “resolved topology”. In the probed mass regime, the heavy neutrinos are produced with large transverse momentum (i.e. are highly boosted) and their decay products are very collimated. Therefore a large-radius jet (large- R jet) can be used to reconstruct all or part of the N_R . Since jet construction in ATLAS includes the energy deposition of electrons in the calorimeters but no muons, the analysis strategy is different for the two cases. In the electron channel, the electron energy deposit is included in the constructed large- R jet originating from the decay of the N_R , and the large- R jet can be considered as a proxy for the N_R . In

^{*} E-mail address: atlas.publications@cern.ch.

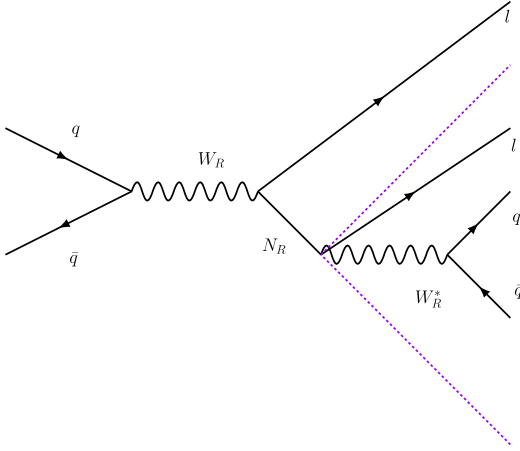


Fig. 1. Diagram of the W_R decay via N_R into charged leptons and quarks. The leptons need to be of the same flavour, but can be the same or opposite charges. The dashed purple lines indicate that the N_R decay products can be inside a large- R jet.

the muon channel, the four-momentum of the muon is added to the large- R jet to obtain the N_R four-momentum. The search is restricted to the scenarios where both leptons have the same flavour. No constraint on their charge is enforced, because of the higher probability of charge misidentification for high- p_T electrons.

The results obtained in this search are also applicable to other variations of the LRSM that contain a right-handed gauge boson and neutral leptons, such as inverse seesaw models [21]. Additionally, this search is also applicable to R-parity-violating supersymmetry [22,23], where a selectron is resonantly produced and subsequently decays into an electron and a neutralino, and the latter decays to a lepton and quarks through a non-zero λ' coupling. When the neutralino is boosted, its decay products can be reconstructed as a single large- R jet [24], analogous to the final state probed in this analysis.

2. ATLAS detector

The ATLAS detector [25] at the Large Hadron Collider (LHC) is a multipurpose particle detector with a forward-backward symmetric cylindrical geometry and a near 4π coverage in solid angle.¹ It consists of an inner tracking detector (ID) surrounded by a thin superconducting solenoid providing a 2 T axial magnetic field, electromagnetic (EM) and hadronic calorimeters, and a muon spectrometer (MS). The ID consists of silicon pixel, silicon microstrip, and straw-tube transition-radiation tracking detectors, covering the pseudorapidity range $|\eta| < 2.5$. The calorimeter system covers the pseudorapidity range $|\eta| < 4.9$. Electromagnetic calorimetry is provided by barrel and endcap high-granularity lead and liquid-argon (LAr) sampling calorimeters, within the region $|\eta| < 3.2$. There is an additional thin LAr presampler covering $|\eta| < 1.8$, to correct for energy loss in material upstream of the calorimeters.

For $|\eta| < 2.5$, the LAr calorimeters are divided into three layers in depth. Hadronic calorimetry is provided by a steel/scintillator-tile calorimeter, segmented into three barrel structures within $|\eta| < 1.7$, and two copper/LAr hadronic endcap calorimeters, which cover the region $1.5 < |\eta| < 3.2$. The forward solid angle up to $|\eta| = 4.9$ is covered by copper/LAr and tungsten/LAr calorimeter modules, which are optimised for energy measurements of electrons/photons and hadrons, respectively. The muon spectrometer is the outermost layer of the detector, and is designed to measure muons up to $|\eta|$ of 2.7. It comprises separate trigger and high-precision tracking chambers that measure the deflection of muons in a magnetic field generated by superconducting air-core toroids. The muon trigger chambers cover up to $|\eta|$ of 2.4.

The ATLAS detector selects events using a tiered trigger system [26]. The first level is implemented in custom electronics and reduces the event rate from the bunch-crossing frequency of 40 MHz to a design value of 100 kHz. The second level is implemented in software, running on a general-purpose processor farm which processes the events and reduces the rate of recorded events to about 1 kHz.

3. Data and simulation samples

This analysis uses proton-proton (pp) collision data at a centre-of-mass energy $\sqrt{s} = 13$ TeV collected in 2015, 2016 and 2017 that satisfy a number of data-quality criteria. The amount of data used in this analysis corresponds to an integrated luminosity of 80 fb^{-1} .

Simulated signal and background events are used to optimise the event selection, to validate the performance of large- R jets containing an electron, evaluate the Z +jets background contribution, and calculate signal yields and their systematic uncertainties. Signal events were simulated at leading order (LO) in QCD using MG5_aMC@NLO 2.2.2 [27], with PYTHIA 8.186 [28] using the NNPDF23LO [29] parton distribution function (PDF) set and the A14 set of tuned parameters (tune) [30] for parton showering and hadronisation. A version of a LRSM model produced with FeynRules [31] was implemented [32] in MG5_aMC@NLO and further modified by the authors of Refs. [33,34]. This model assumes the equivalence of left and right-handed weak gauge couplings, universality of all the right-handed quarks and right-handed leptons, and the same masses for all three flavours of heavy right-handed neutrinos. Events were generated without constraints on the charge of leptons, in line with the production of Majorana neutrinos. Signal samples were generated for different m_{W_R} and m_{N_R} hypotheses, covering the range of 3–6 TeV for m_{W_R} and 150–600 GeV for m_{N_R} . The production cross-sections are scaled to next-to-leading order (NLO) in QCD following Ref. [35].

The background processes considered are top-quark pairs ($t\bar{t}$), Z/W +jets, single top-quark, diboson and multijet production. Table 1 summarises the generator configurations used to produce the samples. The $t\bar{t}$ sample cross-sections are scaled to next-to-next-to-leading order (NNLO) in perturbative QCD, including soft-gluon resummation to next-to-next-to-leading-log (NNLL) accuracy [36], assuming a top-quark mass $m_t = 172.5$ GeV [37]. The resummation damping parameter, h_{damp} in the POWHEG model, which controls the matching of matrix elements to parton showers and regulates the high- p_T radiation, was set to $1.5m_t$. The single-top-quark and W/Z +jets samples are scaled to the NNLO theoretical cross-sections [38–41].

The MC samples were processed through the full ATLAS detector simulation [50] based on GEANT4 [51], or a faster simulation [52] based on a parameterisation of the calorimeter response and GEANT4 for the other detector systems, and reconstructed and analysed using the same procedure and software as used for the data. The signal modelling is found to be consistent between the

¹ ATLAS uses a right-handed coordinate system with its origin at the nominal interaction point (IP) in the centre of the detector and the z -axis along the beam pipe. The x -axis points from the IP to the centre of the LHC ring, and the y -axis points upwards. Cylindrical coordinates (r, ϕ) are used in the transverse plane, ϕ being the azimuthal angle around the z -axis. The pseudorapidity is defined in terms of the polar angle θ as $\eta = -\ln \tan(\theta/2)$. The angular separation between two objects is defined as $\Delta R \equiv \sqrt{(\Delta\eta)^2 + (\Delta\phi)^2}$, where $\Delta\eta$ and $\Delta\phi$ are the separations in η and ϕ . The rapidity is defined as $y = \frac{1}{2} \ln \frac{E+p_z}{E-p_z}$, where E is the energy and p_z is the longitudinal component of the momentum along the beam pipe. The angular separation between two objects in terms of rapidity is defined as $\Delta R_y \equiv \sqrt{(\Delta y)^2 + (\Delta\phi)^2}$, where Δy and $\Delta\phi$ are the separations in y and ϕ . Momentum in the transverse plane is denoted by p_T .

Table 1

Main features of the Monte Carlo models used to simulate background samples. Top quark refers to both the $t\bar{t}$ and single-top processes. ME and PS refer to matrix element and parton shower, while leading order (LO) and next-to-leading order (NLO) indicate the accuracy of the generators in perturbative QCD (pQCD). For PowHEG + Pythia8, different PDF sets were used in ME and PS.

Process	Top quark	W + jets	Z + jets	Diboson	Multijet
Generator	PowHEG [42–45] + Pythia8	PowHEG + Pythia8	Sherpa [46]	Pythia8	
ME order in pQCD	NLO	NLO	NLO	LO	
Version	v2, 8.186	v2, 8.186	2.2.1	8.186	
PDF (ME, PS)	NNPDF30NLO [47], NNPDF23LO	CT10 [48], CTEQ6L1	NNPDF30NNLO	NNPDF23LO	
PS tune	A14	AZNLO [49]	Default	A14	

full and the fast simulation, after application of dedicated calibration procedures. To simulate the effects of additional collisions in the same and neighbouring bunch crossings (pile-up), additional minimum-bias events generated using Pythia8 with the A3 tune [53] and MSTW2008 [54] PDF set were overlaid onto the signal and background simulated events, with a distribution of the number of collisions matching that of the data. To account for the differences in particle reconstruction, trigger, identification and isolation efficiencies between simulation and data, correction factors are derived in dedicated measurements and applied to the simulated events.

4. Event selection and characterisation

The event selection is designed to select signal events, while rejecting background events, based on the signal topology. The events are selected if they contain exactly two same-flavour leptons (with no charge requirement) and at least one trimmed large- R jet [55] with large transverse momentum $p_T > 200$ GeV. The highest- p_T (leading) lepton should be back-to-back in azimuth with the large- R jet, while other (subleading) lepton should be contained in the large- R jet. In Fig. 2, the reconstructed p_T distributions of the leading and subleading lepton, as well as of the selected large- R jet, and the candidate N_R mass are shown for four representative signal samples. The leading electron and the large- R jet are balanced in p_T , with the maxima at roughly half of the corresponding m_{W_R} values. The leading muon p_T shows the same characteristic, but the p_T of the large- R jet is lower and has a broader distribution, as it does not contain the energy from the subleading muon, and the muon p_T resolution for high- p_T muons is worse. The reconstructed mass of the N_R in each case is consistent with the expected value. The natural width of the resonance varies with the mass and is 100 GeV for $m_{W_R} = 3$ TeV. At this mass the width of the reconstructed mass peak is about 150 GeV in the electron channel, and about 350 GeV in the muon channel.

The detailed selection criteria are listed in Table 2 and further discussed below. Events with electrons and muons are analysed separately. The leading lepton is required to pass a single-lepton trigger. For data collected in 2015, the lowest p_T trigger threshold is 24 GeV and 20 GeV for single-electron and single-muon triggers, respectively. For 2016 and 2017 data, the threshold is 26 GeV for both.

Electron candidates are reconstructed from an isolated energy deposit in the electromagnetic calorimeter matched to an ID track, within the fiducial region of transverse energy $p_T > 26$ GeV and $|\eta| < 2.47$. Candidates within the transition region between the barrel and endcap electromagnetic calorimeters, $1.37 < |\eta| < 1.52$, are excluded. Muon candidates are reconstructed by combining tracks found in the ID with tracks found in the muon spectrometer and are required to satisfy $p_T > 28$ GeV and $|\eta| < 2.5$. Electrons and muons are required to be isolated using criteria based on tracks and calorimeter energy deposits. For track-based isolation, the discriminating variable is the scalar sum of the p_T of tracks

coming from the primary vertex ² in a variable-size cone around the lepton direction (excluding the track identified as the lepton), with the cone size given by the maximum of $\Delta R = 10 \text{ GeV}/p_T^\ell$ and R_0 , where p_T^ℓ is the p_T of the lepton, and R_0 is a constant, set to 0.2 for electrons, and 0.3 for muons. For calorimeter-based isolation, the discriminating variable is the sum of the transverse energies of topological clusters [56] around the lepton in a cone of size $\Delta R = 0.2$.

The inputs to the jet construction are noise-suppressed three-dimensional topological clusters of energy deposits in the calorimeters, built from calorimeter cells [56]. They are classified as either electromagnetic or hadronic, based on their shape, depth and energy density. The energy clusters are calibrated to the hadronic scale. The momenta of the jets are corrected for energy losses in passive material and for the non-compensating response of the calorimeter [57]. The large- R jets are constructed with the anti- k_t algorithm [58] with a radius parameter of $R = 1.0$, through its implementation in FastJet [59]. They are further trimmed [55] to reduce the contamination from soft uncorrelated radiation. In this method, the original constituents of the jets are reclustered using the k_t algorithm [60] with a radius parameter $R_{\text{sub}} = 0.2$ in order to produce a collection of subjets. These subjets are discarded if they carry less than a specific fraction ($f_{\text{cut}} = 5\%$) of the p_T of the original jet. The remaining constituents are summed to form the four-momentum of the final jet.

In the electron channel, the large- R jets are required to have a mass of at least 50 GeV, while no such requirement is applied in the muon channel. This is because in the former case, the large- R jet includes the electron, while in the muon channel, the muon is not included in the large- R jet.

Small-radius jets constructed with the anti- k_t algorithm using energy clusters calibrated to the electromagnetic scale with a radius parameter of $R = 0.4$ are used to check for possible overlap between objects, and to perform b -tagging (described in Section 5). In the muon channel, the event is discarded if either muon satisfies $\Delta R_y(\mu, \text{jet}) < \min(0.4, 0.04 + 10 \text{ GeV}/p_T^\mu)$, in order to avoid jets formed from energy deposits associated to high energy muons. In the electron channel, for the leading electron, first all small-radius jets within $\Delta R_y = 0.2$ of a selected electron are removed. Then the event is discarded if the leading electron is within $\Delta R_y = 0.4$ of a remaining small-radius jet. This is referred to as the nominal overlap removal procedure for electrons. A modified procedure, described in Section 5, is applied for the subleading electron as, unlike muons, electron clusters can overlap with a jet and the signal efficiency drops off if the standard overlap removal approach is followed.

Further requirements based on the characteristics of the signal are applied:

² Collision vertices are formed from tracks with $p_T > 400$ MeV. If an event contains more than one vertex candidate, the one with the highest $\sum p_T^2$ of its associated tracks is selected as the primary vertex.

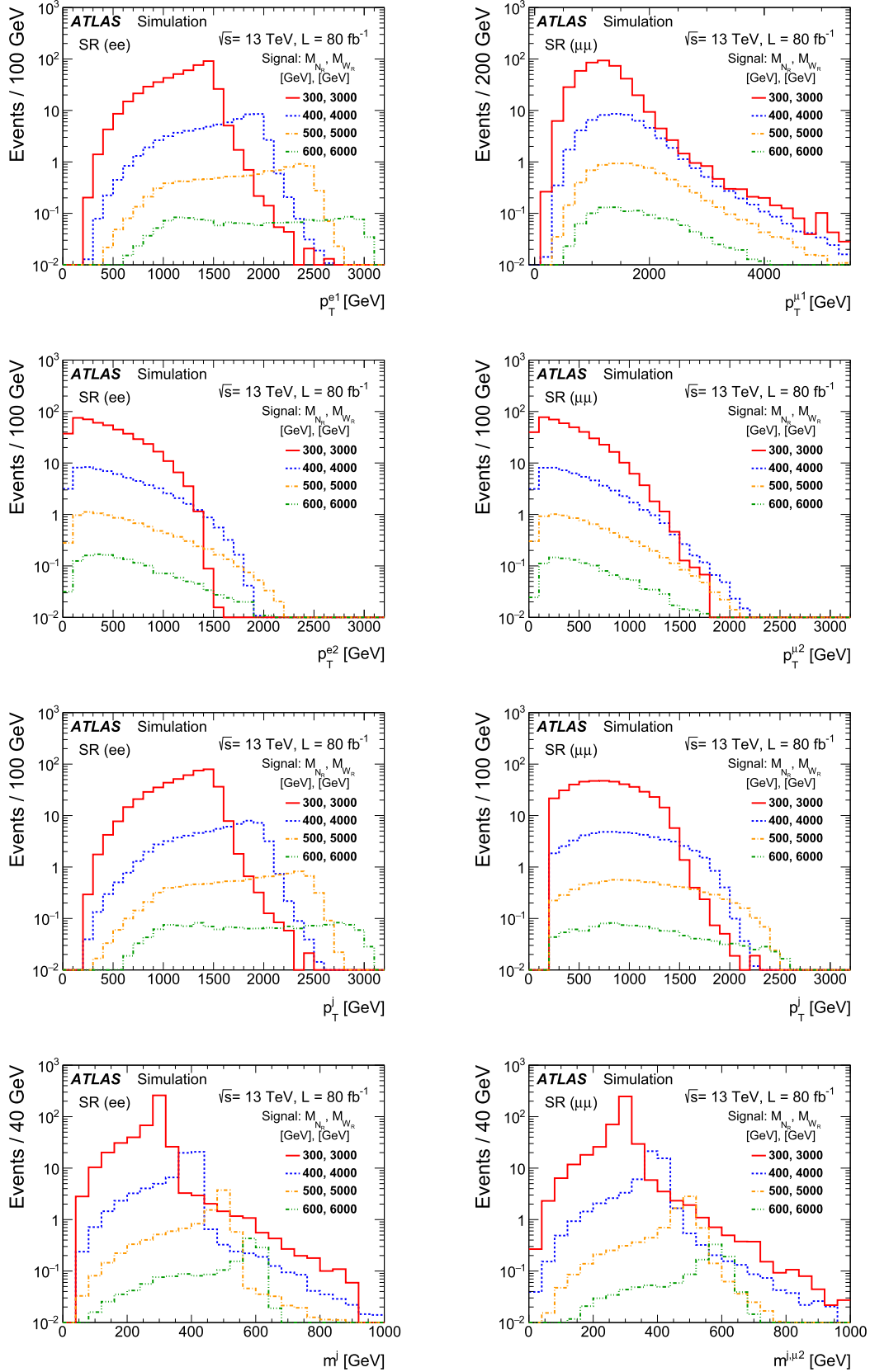


Fig. 2. Reconstructed distributions of the transverse momentum of the leading lepton, subleading lepton, the selected large- R jet, and the N_R candidate mass in electron (left column) and muon (right column) channels for four representative signal samples in the signal region. The indices 1 and 2 indicate leading and subleading lepton, respectively.

Table 2

Object selection criteria. The significance of the transverse impact parameter is defined as the transverse impact parameter d_0 divided by its uncertainty, σ_{d_0} , of tracks relative to the primary vertex with the highest sum of track p_T . The longitudinal impact parameter z_0 is multiplied by $\sin\theta$, where θ is the polar angle of the track.

	Electron channel	Muon channel
Lepton:		
p_T	> 26 GeV	> 28 GeV
$ \eta $	$ \eta < 1.37$ or $1.52 < \eta < 2.47$	< 2.5
Leading lepton quality	Medium [61], isolated [61]	Medium [62], isolated [62]
Subleading lepton quality	Medium, no isolation	Medium, no isolation
Transverse impact parameter significance	$ d_0 /\sigma_{d_0} < 5.0$	$ d_0 /\sigma_{d_0} < 3.0$
Longitudinal impact parameter	$ z_0 \sin\theta < 0.5$ mm	
Trimmed large-R jet:		
p_T	> 200 GeV	
$ \eta $	< 2.0	
Mass	> 50 GeV	None

- ΔR_y between the subleading lepton and the large-R jet is required to be less than 1, in order for the lepton to be inside the jet.
- $\Delta\phi$ between the leading lepton and the large-R jet is required to be greater than 2, in order to have a balanced topology between the N_R and the lepton from the W_R decay.
- In order to reduce the Z +jets background, events with a dilepton invariant mass of less than 200 GeV are vetoed, and the $\Delta\phi$ between the leading and subleading leptons is required to be greater than 1.5.

After applying these requirements, simulation studies show that the background consists mainly of $t\bar{t}$ and Z +jets processes (including off-shell Z/γ^* production), while contributions from W +jets, single-top-quark and multijet processes are negligible. No requirements on b -tagged jets are applied, as the W_R in the signal can decay to a top and bottom quark pair.

The final discriminating observable used in the analysis is the reconstructed mass of the W_R candidate, $m_{W_R}^{\text{reco}}$. In the electron channel, the selected large-R jet corresponds to the N_R candidate, and therefore the W_R candidate four-momentum is obtained by adding the large-R jet and the leading electron four-momenta. In the muon channel, the N_R candidate four-momentum is obtained by adding the four-momentum of the selected large-R jet to that of the muon contained in the jet. The W_R candidate four-momentum is obtained by adding the N_R candidate four-momentum to that of the leading muon. In both cases, if there is more than one large-R jet in the event, the large-R jet with the largest mass is used.

Based on the range of $m_{W_R}^{\text{reco}}$, control and signal regions (CR, SR) are defined as specified in Table 3. The CR is defined in a region of low reconstructed $m_{W_R}^{\text{reco}}$ corresponding to a parameter space excluded by previous searches [14]. The background in the SR is evaluated from a combined fit of MC and data events in the CR (described in Section 6). To test the performance of large-R jets containing electrons, a validation region (VR) is defined with a selection orthogonal to the CR and the SR. This requires a muon balanced in p_T by a large-R jet with an electron inside. By construction, the VR is dominated by $t\bar{t}$ events decaying dileptonically to $e\mu$ final states.

In Fig. 3, good agreement is observed between data and simulation in the $m_{W_R}^{\text{reco}}$ distributions in the control regions of the electron and muon channels, as well as in the validation region. In the bottom-right plot, the selection efficiency times acceptance is shown for different signal samples. The efficiency decreases for lower m_{N_R} and higher m_{W_R} values. The largest inefficiency arises from the difficulty of electron reconstruction close to hadronic activity, which is discussed in the next section. The probability of producing an off-shell W_R increases with the mass. This can result

Table 3

Definition of signal, control and validation regions.

Region	Range of $m_{W_R}^{\text{reco}}$	Lepton flavour
Signal region (SR)	> 2 TeV	Same flavour
Control region (CR)	< 2 TeV	Same flavour
Validation region (VR)	All	Mixed flavour (leading: muon; subleading: electron)

in a less boosted N_R , explaining the drop in signal efficiency for higher m_{W_R} values.

5. Performance of large-R jets containing electrons

A distinguishing feature of this search is the use of large-R jets containing electrons as a proxy for N_R in the electron channel. Since the large-R jet construction procedure is based on energy clusters calibrated at the hadronic scale, the effect of a non-negligible fraction of EM clusters in the large-R jet needs to be investigated. The analysis does not use the kinematic properties of the identified electron inside the large-R jets to reconstruct the N_R or W_R invariant masses, but uses the mass of the large-R jet, which includes the associated electron clusters. The presence of real hadronic activity close to an electron may affect the reconstruction of the electron.

The jet mass and energy scales, JMS and JES, defined as the average of the ratio of the mass or energy of the reconstructed and corresponding generator-level large-R jets, are used to study the effect of including the large EM-cluster of the electron in the jet reconstruction. The matching between detector-level and generator-level large-R jets is performed with $\Delta R_y < 0.75$. The generator-level jet is obtained by clustering stable final-state particles (with lifetime greater than 30 ps) except muons and neutrinos using the same jet algorithm, radius parameter and trimming used at the detector-level. The JMS and JES of the selected large-R jets for a few representative signal samples are shown in Fig. 4 as a function of the ratio of the energy of the electron to the energy of the large-R jet. This ratio can be considered a proxy for the electromagnetic energy fraction in the large-R jet. Constant values of JES and JMS within a few percent of unity indicate that the large-R jet has only a weak dependence on the fraction of electromagnetic energy inside the jet, and thus no particular additional corrections are required for the signal large-R jets. Typical numbers for the large-R jet mass resolution (JMR) in signal events are about 4-6% in the electron channel and about 7-14% in the muon channel, while the large-R jet energy resolution (JER) is about 3-5% GeV in both channels. As opposed to the muon channel, in the electron channel the large-R jet does contain the electron as a compact and high energy deposit. This implies a more precise angular distribu-

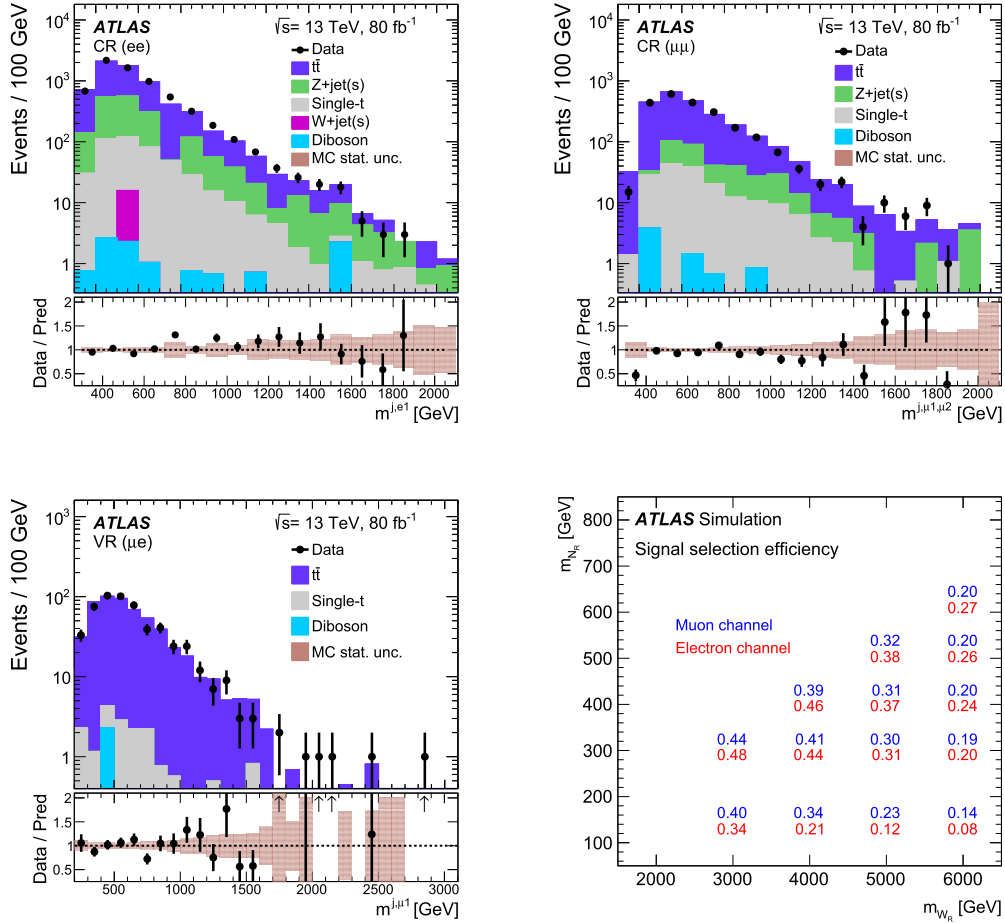


Fig. 3. Distributions of the reconstructed mass of the W_R , in the electron (top left), muon (top right) channel control regions, in the validation region (bottom left), and the signal selection efficiency for a number of benchmark points (bottom right) using simulated signal samples. The $m_{W_R}^{\text{reco}}$ distributions only include statistical uncertainties, which are shown for both the data and simulation in the ratios.

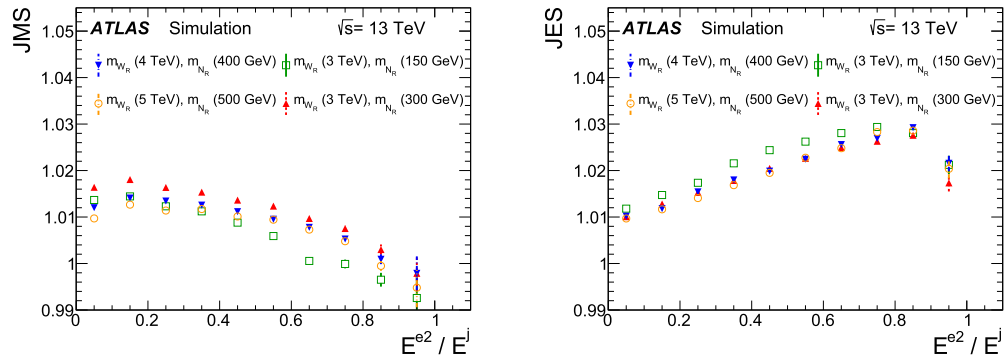


Fig. 4. Large- R jet average JMS (left) and JES (right) as a function of subleading electron energy divided by the large- R jet energy for signal samples.

tion of the energies in the jet and thus a better JMR in the electron channel.

In signal events, as almost all selected large- R jets contain activity from both the W_R hadronic decay and the nearby electron, application of the nominal overlap removal procedure, as described in Section 4, for the subleading electron results in a large loss of signal efficiency. However, it is observed that removing events where the electron and the nearest jet are within $\Delta R_y < 0.04$ retains a sizeable fraction of the signal events and rejects a large fraction of the background events. The discarded events are dominated by the case where isolated electrons are reconstructed as jets.

A study is performed to check the validity of the electron efficiency correction factors, which account for potential differences in electron reconstruction, identification and isolation efficiency between data and simulation and are derived using well-isolated electrons [61]. A sample of $t\bar{t}$ events decaying into a mixed-flavour dileptonic final state is chosen. The leading lepton is chosen to be a muon with nominal isolation requirements, and the subleading lepton is chosen to be an electron with no isolation requirements. The rest of the selection is the same as the signal selection, except that the events are selected with at least one b -tagged small-radius jet. The b -tagging is based on a multivariate algorithm [63]. Several observables based on the long lifetime of b -hadrons and the

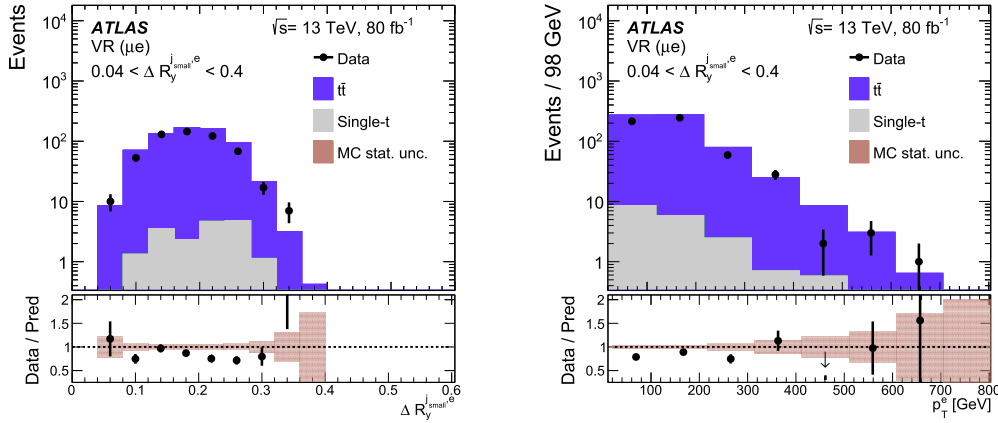


Fig. 5. Angular separation between the subleading electron and nearest small-radius jet (left) and transverse momentum distribution of the subleading electron (right) in events with a leading muon and subleading electron, requiring one b -tagged small-radius jet. The distributions only include statistical uncertainties, which are shown for both the data and simulation in the ratios.

b - to c -hadron decay topology, are used as algorithm input to discriminate between b -jets, c -jets and other jets. The b -tagging requirement corresponds to the 70% efficient working point for b -jets, as determined in simulated $t\bar{t}$ events, while the rejection rates of τ -jets, c -jets and light-flavour jets are 55, 12 and 381, respectively [64,65].

The large- R jet requirements are the same as in the nominal selection. Only the events in which the electrons and the nearest small-radius jet are within $0.04 < \Delta R_j < 0.4$ are studied. The distributions of electron p_T and ΔR_j between the electron and the small-radius jet show satisfactory agreement between data and simulation, as shown in Fig. 5. An additional uncertainty of 30% on the electron efficiency for electrons within $0.04 < \Delta R_j < 0.4$ is derived from the difference in yields between data and the simulation, statistical uncertainties as well as the theoretical and b -tagging uncertainties on the simulation.

6. Background estimation and systematic uncertainty

While the CR is dominated by $t\bar{t}$ events, the fraction of Z +jets events becomes larger at higher masses as they have a less steeply falling mass distribution than $t\bar{t}$ events, as shown in Fig. 3. In order to take this into account in evaluating the background in the SR, which is located at higher masses, a data-driven approach is used to evaluate the $t\bar{t}$ contribution in conjunction with a fitted MC prediction of the Z +jets background. The fit to the data in the CR is extrapolated to the SR.

Different steeply falling functions are tested, motivated by Refs. [66,67], where they are found to fit steeply falling distributions like the scalar sum of jet transverse momenta in multijet events or the dijet mass. It is observed that the functional form $A \exp(-Bu)/u^C$ describes the data distribution in the CR the best, while the functional form $A'(1-u)^{B'}(1+u)^{C'u}$ best describes the Z +jets MC distribution. In both cases, $u = m_{W_R}^{\text{reco}}/\sqrt{s}$ and the choice of fit function is determined by the goodness of fit (based on the χ^2 per degree of freedom) as well as by the best agreement with the yields from the MC background estimate in the CR. First, the fit parameters A' , B' , and C' are determined from Z +jets MC using a reconstructed $m_{W_R}^{\text{reco}}$ range of 400–4000 GeV, then the fit to data is performed using the function $A \exp(-Bu)/u^C + A'(1-u)^{B'}(1+u)^{C'u}$, to determine the values of the parameters A , B and C . This functional form is fitted in the CR range of 600–1800 GeV, where the range is chosen depending on the goodness of the fits. The slope of the background fit is steeper in the muon channel compared to the electron channel.

In the VR the fit performed for reconstructed W_R candidate masses 600–1800 GeV is extrapolated into the region > 2 TeV and the fit prediction is compared to the data yield finding consistency. In order to assess the systematic uncertainty related to the $t\bar{t}$ data-driven fit, variations of the data fit range are made, and the largest change in the SR yield obtained from these variations is taken as the uncertainty. The same is done for the Z +jets MC fit, and the uncertainty is added in quadrature to the uncertainty derived from fitting alternative Z +jets MC samples obtained after varying the scale (by factors of two and one half) and using alternative PDF sets [14]. This uncertainty is larger than the difference yield obtained using POWHEG + PYTHIA8. The relative uncertainty of the background yield in the SR is about 25% for both channels. Statistical uncertainties on the fits are estimated using pseudo-experiments built by varying the input data points within their statistical uncertainties. The resultant background fit, along with the estimated uncertainty is shown in Fig. 6.

7. Systematic uncertainties of the signal yield

Systematic uncertainties affect the shape and normalisation of the $m_{W_R}^{\text{reco}}$ distributions, thereby changing the signal yield. The dominant uncertainties in the SR are shown in Table 4. They can be classified as originating from experimental or theoretical sources.

The yields from simulated samples are affected by uncertainties related to the description of the detector response. The dominant uncertainty is related to the electron and muon identification, which is (4–20)% in the electron channel (including the additional 30% uncertainty for electrons reconstructed nearby a small-radius jet) and (4–8)% in the muon channel, depending on the values of m_{W_R} and m_{N_R} . The uncertainties related to the electron trigger, reconstruction, and isolation are (4–5)%. The uncertainties related to the muon trigger and isolation are about 1%. These uncertainties are assessed by comparing data and simulation samples of $Z \rightarrow \ell^+ \ell^-$ decays [62,61]. The simulation is used to extrapolate to lepton p_T beyond a few hundred GeV. The other uncertainties such as those related to JES and JMS of the large- R jets are evaluated by comparing the ratio of calorimeter-based to track-based measurements in multijet events in data and simulation [68,69,57]. The uncertainties related to JMR and JER modelling are evaluated by increasing the nominal resolution by 20% [70] and 2% respectively. These uncertainties are at sub-percent level. The average number of interactions per bunch crossing is rescaled to improve the agreement of simulation with data, and the corresponding uncertainty, as large as the correction, has an effect of 0.5% in the

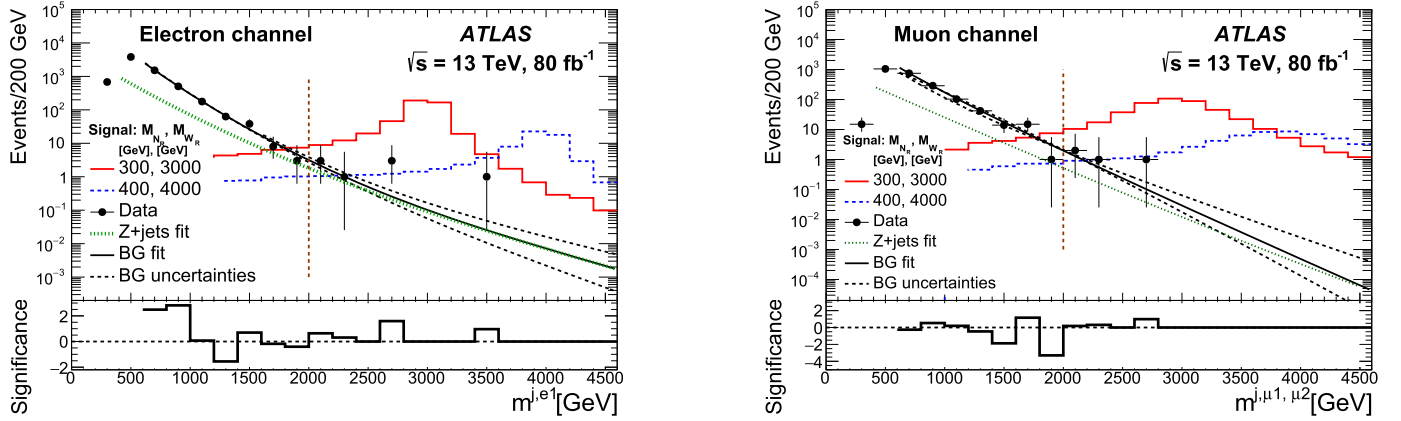


Fig. 6. Comparison of the m_W^{reco} distribution between data and the fitted background prediction for the electron (left) and muon (right) channels. Two signal scenarios considered in this search are overlaid. The dashed brown lines at 2 TeV show the boundary between the CR and SR. The dashed black lines depict the uncertainty on the background fit. The solid black lines on the data points indicate the Poisson uncertainties. The significance, which indicates the deviation of data in each bin from the background fit, is computed as the difference between the observed data and fit values, divided by the square root of the observed data value.

Table 4

Relative systematic uncertainties of the signal yield in the signal region, in percentage for each source. The ranges indicate the different signal samples. The systematic uncertainties with sub-percent contributions are not shown.

Component	Electron channel (%)	Muon channel (%)
Lepton identification	4–20	4–8
Lepton isolation	4–5	1.0–1.5
Lepton reconstruction	4–5	1–4
Lepton trigger	4–5	0.5
Pile-up	<0.5	2–3
Luminosity	2	2
Theory	10	10

electron channel, and up to 3% in the muon channel, caused by the lack of a large- R jet mass threshold in the latter case. The uncertainty in the 2015, 2016 and 2017 integrated luminosity is 2%. It is derived from the calibration of the luminosity scale using x - y beam-separation scans, following a methodology similar to that detailed in Ref. [71], and using the LUCID-2 detector for the baseline luminosity measurements [72].

The theory uncertainty of the signal yield is evaluated by varying the renormalisation and factorisation scales by factors of 2 and 0.5, and using alternative PDF sets, CTEQ6L1 [73] and MSTW2008LO [54] via SysCalc [74]. The dominant effect on the yield comes from the scale variation. The total effect on the signal yield is at most 10%. The uncertainties on the background yield are described in Section 6.

8. Results

Fig. 6 shows the m_W^{reco} distributions in the SR for the electron and muon channels. In order to search for the presence of a massive resonance, yields from simulated signal samples and the data-driven background estimate (corresponding to $m_W^{\text{reco}} > 2$ TeV) are fit to the data, separately in the electron and muon channels, using a single bin covering the entire SR. The integral of the background functional shape in the SR is used to evaluate the expected background, as shown in Table 5. The statistical analysis is based on a likelihood fit to data. The likelihood is constructed using a single-bin Poissonian counting-experiment approach based on the RootStats framework [75,76]. The uncertainties of the background yield are incorporated as Gaussian constraints in the likelihood itself in terms of a set of nuisance parameters.

The compatibility of the observed data with the background-only hypothesis is tested by fitting the data with the background

Table 5

Observed yields and expected background yields in the signal region. The significance and the p -values are shown for the background-only hypothesis. Expected yields from three representative signal samples are also shown.

	Electron channel	Muon channel
Signal ($m_{W_R} = 3$ TeV, $m_{N_R} = 150$ GeV)	346^{+48}_{-75}	411^{+36}_{-48}
Signal ($m_{W_R} = 3$ TeV, $m_{N_R} = 300$ GeV)	471^{+42}_{-69}	429^{+29}_{-40}
Signal ($m_{W_R} = 4$ TeV, $m_{N_R} = 400$ GeV)	66^{+6}_{-10}	57^{+4}_{-4}
Expected background	$2.8^{+0.5}_{-0.7}$	$1.9^{+0.5}_{-0.7}$
Observed events	8	4
Significance	2.4σ	1.2σ
p -value	0.0082	0.12

model to obtain the p -value. The significance of an excess can be quantified by the probability (p -value) that a background-only experiment is more signal-like than observed. The p -values are given in Table 5. In the electron channel, 8 events are observed, while the expected background is $2.8^{+0.5}_{-0.7}$ events. In the muon channel 4 events are observed, while the expected background is $1.9^{+0.5}_{-0.7}$ events. The observed significance corresponds to 2.4σ in the electron channel and 1.2σ in the muon channel.

Lower limits on the masses of N_R and W_R for each of the considered signal scenarios are determined by using the profiled likelihood test statistic [77] with the CL_s method [78,79]. The inputs to the limit calculations are the signal cross-sections and the signal efficiencies in the m_{W_R} - m_{N_R} grid. A linear interpolation between several benchmark samples in the m_{W_R} range 3–6 TeV and in the m_{N_R} range 0.1–1.8 TeV is performed. The results are shown in Fig. 7, separately for electron and muon channels. The CL_s is computed using pseudo-experiments. The data statistical uncertainty has a significantly larger impact on the limits than the systematic uncertainties. The leading systematic uncertainty is the background modelling uncertainty and, in the case of the W_R and N_R mass limits, the signal theory uncertainties or the electron identification uncertainty, depending on the signal mass values.

The excluded region extends to m_{W_R} of 4.8 TeV in the electron channel and to 5 TeV in the muon channel, for m_{N_R} of 0.4–0.5 TeV where the search is most sensitive. For m_{N_R} of 1.8 TeV the excluded m_{W_R} is 4 TeV in both channels. The limits in the electron channel are weaker compared to those in the muon channel for low m_{N_R} values, as the electron reconstruction and identification efficiency is lower for these W_R , N_R mass configurations. For higher m_{N_R} values, the worsening muon resolution and reconstruction efficiency result in weaker limits in the muon channel. The exclusion con-

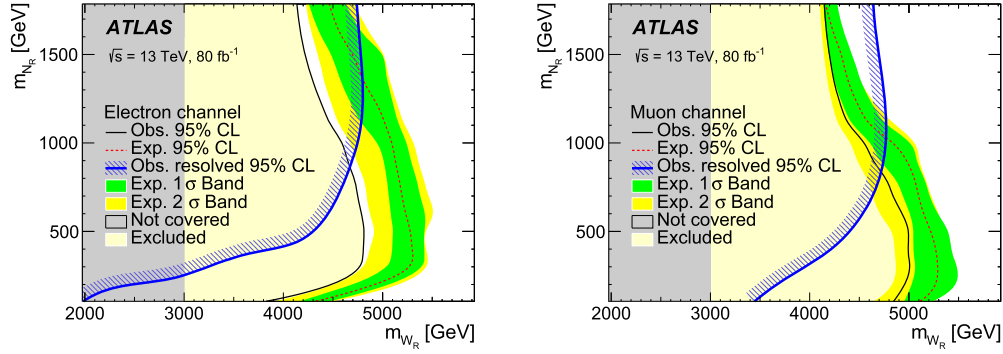


Fig. 7. Observed (black solid line) and expected (red dashed line) 95% CL exclusion contours in the (m_{W_R}, m_{N_R}) plane, along with the $\pm 1\sigma$ and $\pm 2\sigma$ uncertainty bands (green and yellow) around the expected exclusion contour in the electron (left) and muon (right) channels. The exclusion limits in the resolved topology [14] are shown by the blue line.

tour for the resolved topology [14] is overlaid for both channels in Fig. 7, to indicate the complementarity of the present analysis, as lower values of m_{N_R} are excluded.

As the analysis is a single-bin Poissonian counting experiment, the limits on the cross-section are only sensitive to the efficiencies of each signal, and do not depend significantly on m_{W_R} and m_{N_R} . The observed limits on the number of selected signal events are 13.3 events for the electron channel and 8.1 for the muon channel. The corresponding expected limits are 5.4 events for the electron channel and 4.9 for the muon channel.

9. Summary

A search for a heavy right-handed W_R boson decaying into a boosted right-handed neutrino N_R is presented using 80 fb^{-1} of $\sqrt{s} = 13 \text{ TeV}$ proton–proton collision data recorded by the ATLAS detector at the LHC. Both electron and muon final states are analysed for the decay into two same-flavour leptons, $W_R \rightarrow N_R \ell$, $N_R \rightarrow \ell + \text{jets}$. In the electron final state, the analysis makes use of a large- R jet containing an electron as a proxy for N_R , while in the muon channel, the muon four-momentum is added to the large- R jet four-momentum. The observed $m_{W_R}^{\text{reco}}$ spectrum is consistent with the background prediction and exclusion limits at 95% confidence level are set on the N_R masses as a function of the W_R masses. The excluded region extends to m_{W_R} of 4.8 TeV in the electron channel and to 5 TeV in the muon channel, for m_{N_R} of 0.4–0.5 TeV. The use of large- R jets results in a significant reduction of the background contribution. Due to the signal topology, and a higher integrated luminosity this result represents an increase of the exclusion limits in a complementary parameter space compared with previous results that reconstruct the W_R as two resolved jets.

Acknowledgements

We thank CERN for the very successful operation of the LHC, as well as the support staff from our institutions without whom ATLAS could not be operated efficiently.

We acknowledge the support of ANPCyT, Argentina; YerPhI, Armenia; ARC, Australia; BMWFW and FWF, Austria; ANAS, Azerbaijan; SSTC, Belarus; CNPq and FAPESP, Brazil; NSERC, NRC and CFI, Canada; CERN; CONICYT, Chile; CAS, MOST and NSFC, China; COLCIENCIAS, Colombia; MSMT CR, MPO CR and VSC CR, Czech Republic; DNRF and DNSRC, Denmark; IN2P3-CNRS, CEA-DRF/IRFU, France; SRNSFG, Georgia; BMBF, HGF, and MPG, Germany; GSRT, Greece; RGC, Hong Kong SAR, China; ISF and Benozziyo Center, Israel; INFN, Italy; MEXT and JSPS, Japan; CNRST, Morocco; NWO,

Netherlands; RCN, Norway; MNiSW and NCN, Poland; FCT, Portugal; MNE/IFA, Romania; MES of Russia and NRC KI, Russian Federation; JINR; MESTD, Serbia; MSSR, Slovakia; ARRS and MIZŠ, Slovenia; DST/NRF, South Africa; MINECO, Spain; SRC and Wallenberg Foundation, Sweden; SERI, SNSF and Cantons of Bern and Geneva, Switzerland; MOST, Taiwan; TAEK, Turkey; STFC, United Kingdom; DOE and NSF, United States of America. In addition, individual groups and members have received support from BCKDF, Canarie, CRC and Compute Canada, Canada; COST, ERC, ERDF, Horizon 2020, and Marie Skłodowska-Curie Actions, European Union; Investissements d’Avenir Labex and Idex, ANR, France; DFG and AvH Foundation, Germany; Herakleitos, Thales and Aristeia programmes co-financed by EU-ESF and the Greek NSRF, Greece; BSF-NSF and GIF, Israel; CERCA Programme Generalitat de Catalunya, Spain; The Royal Society and Leverhulme Trust, United Kingdom.

The crucial computing support from all WLCG partners is acknowledged gratefully, in particular from CERN, the ATLAS Tier-1 facilities at TRIUMF (Canada), NDGF (Denmark, Norway, Sweden), CC-IN2P3 (France), KIT/GridKA (Germany), INFN-CNAF (Italy), NL-T1 (Netherlands), PIC (Spain), ASGC (Taiwan), RAL (UK) and BNL (USA), the Tier-2 facilities worldwide and large non-WLCG resource providers. Major contributors of computing resources are listed in Ref. [80].

References

- [1] S. Weinberg, Baryon and lepton nonconserving processes, *Phys. Rev. Lett.* **43** (1979) 1566.
- [2] P. Minkowski, $\mu \rightarrow e\gamma$ at a rate of one out of 10^9 muon decays?, *Phys. Lett. B* **67** (1977) 421.
- [3] T. Yanagida, Horizontal symmetry and masses of neutrinos, *Conf. Proc. C* **7902131** (1979) 95.
- [4] M. Gell-Mann, P. Ramond, R. Slansky, Complex spinors and unified theories, *Conf. Proc. C* **790927** (1979) 315, arXiv:1306.4669 [hep-th].
- [5] M. Magg, C. Wetterich, Neutrino mass problem and gauge hierarchy, *Phys. Lett. B* **94** (1980) 61.
- [6] T.P. Cheng, L.-F. Li, Neutrino masses, mixings, and oscillations in $SU(2) \times U(1)$ models of electroweak interactions, *Phys. Rev. D* **22** (11) (1980) 2860.
- [7] R.N. Mohapatra, G. Senjanovic, Neutrino masses and mixings in gauge models with spontaneous parity violation, *Phys. Rev. D* **23** (1) (1981) 165.
- [8] R. Foot, H. Lew, X.G. He, G.C. Joshi, See-saw neutrino masses induced by a triplet of leptons, *Z. Phys. C* **44** (1989) 441.
- [9] J.C. Pati, A. Salam, Lepton number as the fourth color, *Phys. Rev. D* **10** (1974) 275, Erratum: *Phys. Rev. D* **11** (1975) 703.
- [10] R.N. Mohapatra, J.C. Pati, “Natural” left-right symmetry, *Phys. Rev. D* **11** (1975) 2558.
- [11] G. Senjanovic, R.N. Mohapatra, Exact left-right symmetry and spontaneous violation of parity, *Phys. Rev. D* **12** (1975) 1502.
- [12] W.-Y. Keung, G. Senjanovic, Majorana neutrinos and the production of the right-handed charged gauge boson, *Phys. Rev. Lett.* **50** (19) (1983) 1427.
- [13] ATLAS Collaboration, Search for heavy Majorana neutrinos with the ATLAS detector in pp collisions at $\sqrt{s} = 8 \text{ TeV}$, *J. High Energy Phys.* **07** (2015) 162, arXiv:1506.06020 [hep-ex].

- [14] ATLAS Collaboration, Search for heavy Majorana or Dirac neutrinos and right-handed W gauge bosons in final states with two charged leptons and two jets at $\sqrt{s} = 13$ TeV with the ATLAS detector, *J. High Energy Phys.* 01 (2019) 016, arXiv:1809.11105 [hep-ex].
- [15] CMS Collaboration, Search for heavy neutrinos and W bosons with right-handed couplings in proton-proton collisions at $\sqrt{s} = 8$ TeV, *Eur. Phys. J. C* 74 (2014) 3149, arXiv:1407.3683 [hep-ex].
- [16] CMS Collaboration, Search for heavy neutrinos or third-generation leptoquarks in final states with two hadronically decaying t leptons and two jets in proton-proton collisions at $\sqrt{s} = 13$ TeV, *J. High Energy Phys.* 03 (2017) 077, arXiv:1612.01190 [hep-ex].
- [17] CMS Collaboration, Search for a heavy right-handed W boson and a heavy neutrino in events with two same-flavor leptons and two jets at $\sqrt{s} = 13$ TeV, *J. High Energy Phys.* 05 (2018) 148, arXiv:1803.11116 [hep-ex].
- [18] CMS Collaboration, Search for heavy Majorana neutrinos in same-sign dilepton channels in proton-proton collisions at $\sqrt{s} = 13$ TeV, *J. High Energy Phys.* 01 (2019) 122, arXiv:1806.10905 [hep-ex].
- [19] CMS Collaboration, Search for heavy neutrinos and third-generation leptoquarks in hadronic states of two τ leptons and two jets in proton-proton collisions at $\sqrt{s} = 13$ TeV, *J. High Energy Phys.* 03 (2019) 170, arXiv:1811.00806 [hep-ex].
- [20] M. Mitra, R. Ruiz, D.J. Scott, M. Spannowsky, Neutrino jets from high-mass W_R gauge bosons in TeV-scale left-right symmetric models, *Phys. Rev. D* 94 (2016) 095016, arXiv:1607.03504 [hep-ph].
- [21] A.G. Dias, C.A. de, S. Pires, P.S. Rodrigues da Silva, A. Sampieri, Simple realization of the inverse seesaw mechanism, *Phys. Rev. D* 86 (2012) 035007, arXiv:1206.2590 [hep-ph].
- [22] R. Barbier, et al., R-parity-violating supersymmetry, *Phys. Rep.* 420 (2005) 1, arXiv:hep-ph/0406039.
- [23] ATLAS Collaboration, Search for new phenomena in a lepton plus high jet multiplicity final state with the ATLAS experiment using $\sqrt{s} = 13$ TeV proton-proton collision data, *J. High Energy Phys.* 09 (2017) 088, arXiv:1704.08493 [hep-ex].
- [24] B.C. Allanach, S. Biswas, S. Mondal, M. Mitra, Resonant slepton production yields CMS $eejj$ and $q\bar{q}jj$ excesses, *Phys. Rev. D* 91 (2015) 015011, arXiv:1410.5947 [hep-ph].
- [25] ATLAS Collaboration, The ATLAS experiment at the CERN large hadron collider, *JINST* 3 (2008) S08003.
- [26] ATLAS Collaboration, Performance of the ATLAS trigger system in 2015, *Eur. Phys. J. C* 77 (2017) 317, arXiv:1611.09661 [hep-ex].
- [27] J. Alwall, et al., The automated computation of tree-level and next-to-leading order differential cross sections, and their matching to parton shower simulations, *J. High Energy Phys.* 07 (2014) 079, arXiv:1405.0301 [hep-ph].
- [28] T. Sjostrand, S. Mrenna, P. Skands, A brief introduction to PYTHIA 8.1, *Comput. Phys. Commun.* 178 (2008) 852, arXiv:0710.3820 [hep-ph].
- [29] R.D. Ball, et al., Parton distributions with LHC data, *Nucl. Phys. B* 867 (2013) 244, arXiv:1207.1303 [hep-ph].
- [30] ATLAS Collaboration, ATLAS Pythia 8 tunes to 7 TeV data, ATL-PHYS-PUB-2014-021, <https://cds.cern.ch/record/1966419>, 2014.
- [31] A. Alloul, N.D. Christensen, C. Degrande, C. Duhr, B. Fuks, FeynRules 2.0 – a complete toolbox for tree-level phenomenology, *Comput. Phys. Commun.* 185 (2014) 2250, arXiv:1310.1921 [hep-ph].
- [32] A. Roitgrund, G. Eilam, S. Bar-Shalom, Implementation of the left-right symmetric model in FeynRules, *Comput. Phys. Commun.* 203 (2016) 18, arXiv:1401.3345 [hep-ph].
- [33] A. Maiezza, M. Nemevsek, F. Nesti, Lepton number violation in Higgs decay at LHC, *Phys. Rev. Lett.* 115 (2015) 081802, arXiv:1503.06834 [hep-ph].
- [34] M. Nemevsek, F. Nesti, J.C. Vazquez, Majorana Higgses at colliders, *J. High Energy Phys.* 04 (2017) 114, arXiv:1612.06840 [hep-ph].
- [35] O. Mattelaer, M. Mitra, R. Ruiz, Automated neutrino jet and top jet predictions at next-to-leading-order with parton shower matching in effective left-right symmetric models, arXiv:1610.08985 [hep-ph], 2016.
- [36] M. Czakon, A. Mitov, Top++: a program for the calculation of the top-pair cross-section at hadron colliders, *Comput. Phys. Commun.* 185 (2014) 2930, arXiv:1112.5675 [hep-ph].
- [37] ATLAS Collaboration, Studies on top-quark Monte Carlo modelling for Top2016, ATL-PHYS-PUB-2016-020, <https://cds.cern.ch/record/2216168>, 2016.
- [38] N. Kidonakis, Next-to-next-to-leading-order collinear and soft gluon corrections for t -channel single top quark production, *Phys. Rev. D* 83 (2011) 091503, arXiv:1103.2792 [hep-ph].
- [39] N. Kidonakis, Two-loop soft anomalous dimensions for single top quark associated production with a W - or H -, *Phys. Rev. D* 82 (2010) 054018, arXiv:1005.4451 [hep-ph].
- [40] N. Kidonakis, NNLL resummation for s -channel single top quark production, *Phys. Rev. D* 81 (2010) 054028, arXiv:1001.5034 [hep-ph].
- [41] C. Anastasiou, L.J. Dixon, K. Melnikov, F. Petriello, High precision QCD at hadron colliders: electroweak gauge boson rapidity distributions at NNLO, *Phys. Rev. D* 69 (2004) 094008, arXiv:hep-ph/0312266 [hep-ph].
- [42] P. Nason, A new method for combining NLO QCD with shower Monte Carlo algorithms, *J. High Energy Phys.* 11 (2004) 040, arXiv:hep-ph/0409146 [hep-ph].
- [43] S. Frixione, P. Nason, G. Ridolfi, A positive-weight next-to-leading-order Monte Carlo for heavy flavour hadroproduction, *J. High Energy Phys.* 09 (2007) 126, arXiv:0707.3088 [hep-ph].
- [44] S. Frixione, P. Nason, C. Oleari, Matching NLO QCD computations with parton shower simulations: the POWHEG method, *J. High Energy Phys.* 11 (2007) 070, arXiv:0709.2092 [hep-ph].
- [45] S. Alioli, P. Nason, C. Oleari, E. Re, A general framework for implementing NLO calculations in shower Monte Carlo programs: the POWHEG BOX, *J. High Energy Phys.* 06 (2010) 043, arXiv:1002.2581 [hep-ph].
- [46] T. Gleisberg, et al., Event generation with SHERPA 1.1, *J. High Energy Phys.* 02 (2009) 007, arXiv:0811.4622 [hep-ph].
- [47] R.D. Ball, et al., Parton distributions for the LHC Run II, *J. High Energy Phys.* 04 (2015) 040, arXiv:1410.8849 [hep-ph].
- [48] H.-L. Lai, et al., New parton distributions for collider physics, *Phys. Rev. D* 82 (2010) 074024, arXiv:1007.2241 [hep-ph].
- [49] ATLAS Collaboration, Measurement of the Z/γ^* boson transverse momentum distribution in pp collisions at $\sqrt{s} = 7$ TeV with the ATLAS detector, *J. High Energy Phys.* 09 (2014) 145, arXiv:1406.3660 [hep-ex].
- [50] ATLAS Collaboration, The ATLAS simulation infrastructure, *Eur. Phys. J. C* 70 (2010) 823, arXiv:1005.4568 [physics.ins-det].
- [51] S. Agostinelli, et al., Geant4: a simulation toolkit, *Nucl. Instrum. Methods A* 506 (2003) 250.
- [52] ATLAS Collaboration, The simulation principle and performance of the ATLAS fast calorimeter simulation FastCaloSim, ATL-PHYS-PUB-2010-013, <https://cds.cern.ch/record/1300517>, 2010.
- [53] ATLAS Collaboration, The Pythia 8 A3 tune description of ATLAS minimum bias and inelastic measurements incorporating the Donnachie–Landshoff diffractive model, ATL-PHYS-PUB-2016-017, <https://cds.cern.ch/record/2206965>, 2016.
- [54] A.D. Martin, W.J. Stirling, R.S. Thorne, G. Watt, Parton distributions for the LHC, *Eur. Phys. J. C* 63 (2009) 189, arXiv:0901.0002 [hep-ph].
- [55] D. Krohn, J. Thaler, L.-T. Wang, Jet trimming, *J. High Energy Phys.* 02 (2010) 084, arXiv:0912.1342 [hep-ph].
- [56] ATLAS Collaboration, Topological cell clustering in the ATLAS calorimeters and its performance in LHC Run 1, *Eur. Phys. J. C* 77 (2017) 490, arXiv:1603.02934 [hep-ex].
- [57] ATLAS Collaboration, In situ calibration of large- R jet energy and mass in 13 TeV proton–proton collisions with the ATLAS detector, *Eur. Phys. J. C* 79 (2019) 135, arXiv:1807.09477 [hep-ex].
- [58] M. Cacciari, G.P. Salam, G. Soyez, The anti- k_t jet clustering algorithm, *J. High Energy Phys.* 04 (2008) 063, arXiv:0802.1189 [hep-ph].
- [59] M. Cacciari, G.P. Salam, G. Soyez, FastJet user manual, *Eur. Phys. J. C* 72 (2012) 1896, arXiv:1111.6097 [hep-ph].
- [60] S. Catani, Y.L. Dokshitzer, M.H. Seymour, B.R. Webber, Longitudinally invariant k_{\perp} clustering algorithms for hadron hadron collisions, *Nucl. Phys. B* 406 (1993) 187.
- [61] ATLAS Collaboration, Electron reconstruction and identification in the ATLAS experiment using the 2015 and 2016 LHC proton-proton collision data at $\sqrt{s} = 13$ TeV, arXiv:1902.0465, 2019.
- [62] ATLAS Collaboration, Muon reconstruction performance of the ATLAS detector in proton–proton collision data at $\sqrt{s} = 13$ TeV, *Eur. Phys. J. C* 76 (2016) 292, arXiv:1603.05598 [hep-ex].
- [63] ATLAS Collaboration, Performance of b -jet identification in the ATLAS experiment, *JINST* 11 (2016) P04008, arXiv:1512.01094 [hep-ex].
- [64] ATLAS Collaboration, Expected performance of the ATLAS b -tagging algorithms in Run-2, ATL-PHYS-PUB-2015-022, <https://cds.cern.ch/record/2037697>, 2015.
- [65] ATLAS Collaboration, Optimisation of the ATLAS b -tagging performance for the 2016 LHC Run, ATL-PHYS-PUB-2016-012, <https://cds.cern.ch/record/2160731>, 2016.
- [66] ATLAS Collaboration, Search for strong gravity in multijet final states produced in pp collisions at $\sqrt{s} = 13$ TeV using the ATLAS detector at the LHC, *J. High Energy Phys.* 03 (2016) 026, arXiv:1512.02586 [hep-ex].
- [67] ATLAS Collaboration, Search for new phenomena in dijet events using 37 fb $^{-1}$ of pp collision data collected at $\sqrt{s} = 13$ TeV with the ATLAS detector, *Phys. Rev. D* 96 (2017) 052004, arXiv:1703.09127 [hep-ex].
- [68] ATLAS Collaboration, Performance of jet substructure techniques for large- R jets in proton–proton collisions at $\sqrt{s} = 7$ TeV using the ATLAS detector, *J. High Energy Phys.* 09 (2013) 076, arXiv:1306.4945 [hep-ex].
- [69] ATLAS Collaboration, Jet energy scale measurements and their systematic uncertainties in proton–proton collisions at $\sqrt{s} = 13$ TeV with the ATLAS detector, *Phys. Rev. D* 96 (2017) 072002, arXiv:1703.09665 [hep-ex].
- [70] ATLAS Collaboration, Jet mass resolutions in ATLAS using Run 2 Monte Carlo simulation, ATL-PHYS-PUB-2018-015, <https://cds.cern.ch/record/2631339>, 2018.
- [71] ATLAS Collaboration, Luminosity determination in pp collisions at $\sqrt{s} = 8$ TeV using the ATLAS detector at the LHC, *Eur. Phys. J. C* 76 (2016) 653, arXiv:1608.03953 [hep-ex].
- [72] G. Avoni, et al., The new LUCID-2 detector for luminosity measurement and monitoring in ATLAS, *JINST* 13 (2018) P07017.

- [73] J. Pumplin, et al., New generation of parton distributions with uncertainties from global QCD analysis, *J. High Energy Phys.* 07 (2002) 012, arXiv:hep-ph/0201195.
- [74] A. Kalođeropoulos, J. Alwall, The SysCalc code: a tool to derive theoretical systematic uncertainties, arXiv:1801.08401 [hep-ph], 2018.
- [75] L. Moneta, et al., The RooStats project, PoSACAT 2010 (2010) 057, arXiv:1009.1003 [physics.data-an].
- [76] M. Baak, et al., HistFitter software framework for statistical data analysis, *Eur. Phys. J. C* 75 (2015) 153, arXiv:1410.1280 [hep-ex].
- [77] G. Cowan, K. Cranmer, E. Gross, O. Vitells, Asymptotic formulae for likelihood-based tests of new physics, *Eur. Phys. J. C* 71 (2011) 1554, Erratum: *Eur. Phys. J. C* 73 (2013) 2501, arXiv:1007.1727 [physics.data-an].
- [78] T. Junk, Confidence level computation for combining searches with small statistics, *Nucl. Instrum. Methods A* 434 (1999) 435, arXiv:hep-ex/9902006.
- [79] A.L. Read, Presentation of search results: the CL_s technique, *J. Phys. G* 28 (2002) 2693.
- [80] ATLAS Collaboration, ATLAS computing acknowledgements, ATL-GEN-PUB-2016-002, <https://cds.cern.ch/record/2202407>, 2016.

The ATLAS Collaboration

M. Aaboud^{35d}, G. Aad¹⁰¹, B. Abbott¹²⁸, D.C. Abbott¹⁰², O. Abidinov^{13,*}, A. Abed Abud^{70a,70b}, K. Abeling⁵³, D.K. Abhayasinghe⁹³, S.H. Abidi¹⁶⁷, O.S. AbouZeid⁴⁰, N.L. Abraham¹⁵⁶, H. Abramowicz¹⁶¹, H. Abreu¹⁶⁰, Y. Abulaiti⁶, B.S. Acharya^{66a,66b,n}, B. Achkar⁵³, S. Adachi¹⁶³, L. Adam⁹⁹, C. Adam Bourdarios¹³², L. Adamczyk^{83a}, L. Adamek¹⁶⁷, J. Adelman¹²¹, M. Adersberger¹¹⁴, A. Adiguzel^{12c,ah}, S. Adorni⁵⁴, T. Adye¹⁴⁴, A.A. Affolder¹⁴⁶, Y. Afik¹⁶⁰, C. Agapopoulou¹³², M.N. Agaras³⁸, A. Aggarwal¹¹⁹, C. Agheorghiesei^{27c}, J.A. Aguilar-Saavedra^{140f,140a,ag}, F. Ahmadov⁷⁹, X. Ai^{15a}, G. Aielli^{73a,73b}, S. Akatsuka⁸⁵, T.P.A. Åkesson⁹⁶, E. Akilli⁵⁴, A.V. Akimov¹¹⁰, K. Al Khoury¹³², G.L. Alberghi^{23b,23a}, J. Albert¹⁷⁶, M.J. Alconada Verzini⁸⁸, S. Alderweireldt¹¹⁹, M. Aleksa³⁶, I.N. Aleksandrov⁷⁹, C. Alexa^{27b}, D. Alexandre¹⁹, T. Alexopoulos¹⁰, A. Alfonsi¹²⁰, M. Alhroob¹²⁸, B. Ali¹⁴², G. Alimonti^{68a}, J. Alison³⁷, S.P. Alkire¹⁴⁸, C. Allaire¹³², B.M.M. Allbrooke¹⁵⁶, B.W. Allen¹³¹, P.P. Allport²¹, A. Aloisio^{69a,69b}, A. Alonso⁴⁰, F. Alonso⁸⁸, C. Alpigiani¹⁴⁸, A.A. Alshehri⁵⁷, M.I. Alstaty¹⁰¹, M. Alvarez Estevez⁹⁸, B. Alvarez Gonzalez³⁶, D. Álvarez Piqueras¹⁷⁴, M.G. Alvigi^{69a,69b}, Y. Amaral Coutinho^{80b}, A. Ambler¹⁰³, L. Ambroz¹³⁵, C. Amelung²⁶, D. Amidei¹⁰⁵, S.P. Amor Dos Santos^{140a,140c}, S. Amoroso⁴⁶, C.S. Amrouche⁵⁴, F. An⁷⁸, C. Anastopoulos¹⁴⁹, N. Andari¹⁴⁵, T. Andeen¹¹, C.F. Anders^{61b}, J.K. Anders²⁰, A. Andreazza^{68a,68b}, V. Andrei^{61a}, C.R. Anelli¹⁷⁶, S. Angelidakis³⁸, I. Angelozzi¹²⁰, A. Angerami³⁹, A.V. Anisenkov^{122b,122a}, A. Annovi^{71a}, C. Antel^{61a}, M.T. Anthony¹⁴⁹, M. Antonelli⁵¹, D.J.A. Antrim¹⁷¹, F. Anulli^{72a}, M. Aoki⁸¹, J.A. Aparisi Pozo¹⁷⁴, L. Aperio Bella³⁶, G. Arabidze¹⁰⁶, J.P. Araque^{140a}, V. Araujo Ferraz^{80b}, R. Araujo Pereira^{80b}, C. Arcangeletti⁵¹, A.T.H. Arce⁴⁹, F.A. Arduh⁸⁸, J-F. Arguin¹⁰⁹, S. Argyropoulos⁷⁷, J.-H. Arling⁴⁶, A.J. Armbruster³⁶, L.J. Armitage⁹², A. Armstrong¹⁷¹, O. Arnaez¹⁶⁷, H. Arnold¹²⁰, A. Artamonov^{111,*}, G. Artoni¹³⁵, S. Artz⁹⁹, S. Asai¹⁶³, N. Asbah⁵⁹, E.M. Asimakopoulou¹⁷², L. Asquith¹⁵⁶, K. Assamagan²⁹, R. Astalos^{28a}, R.J. Atkin^{33a}, M. Atkinson¹⁷³, N.B. Atlay¹⁵¹, H. Atmani¹³², K. Augsten¹⁴², G. Avolio³⁶, R. Avramidou^{60a}, M.K. Ayoub^{15a}, A.M. Azoulay^{168b}, G. Azuelos^{109,aw}, A.E. Baas^{61a}, M.J. Baca²¹, H. Bachacou¹⁴⁵, K. Bachas^{67a,67b}, M. Backes¹³⁵, F. Backman^{45a,45b}, P. Bagnaia^{72a,72b}, M. Bahmani⁸⁴, H. Bahrasemani¹⁵², A.J. Bailey¹⁷⁴, V.R. Bailey¹⁷³, J.T. Baines¹⁴⁴, M. Bajic⁴⁰, C. Bakalis¹⁰, O.K. Baker¹⁸³, P.J. Bakker¹²⁰, D. Bakshi Gupta⁸, S. Balaji¹⁵⁷, E.M. Baldin^{122b,122a}, P. Balek¹⁸⁰, F. Balli¹⁴⁵, W.K. Balunas¹³⁵, J. Balz⁹⁹, E. Banas⁸⁴, A. Bandyopadhyay²⁴, Sw. Banerjee^{181,i}, A.A.E. Bannoura¹⁸², L. Barak¹⁶¹, W.M. Barbe³⁸, E.L. Barberio¹⁰⁴, D. Barberis^{55b,55a}, M. Barbero¹⁰¹, T. Barillari¹¹⁵, M-S. Barisits³⁶, J. Barkeloo¹³¹, T. Barklow¹⁵³, R. Barnea¹⁶⁰, S.L. Barnes^{60c}, B.M. Barnett¹⁴⁴, R.M. Barnett¹⁸, Z. Barnovska-Blenessy^{60a}, A. Baroncelli^{60a}, G. Barone²⁹, A.J. Barr¹³⁵, L. Barranco Navarro¹⁷⁴, F. Barreiro⁹⁸, J. Barreiro Guimarães da Costa^{15a}, R. Bartoldus¹⁵³, G. Bartolini¹⁰¹, A.E. Barton⁸⁹, P. Bartos^{28a}, A. Basalae⁴⁶, A. Bassalat^{132,ap}, R.L. Bates⁵⁷, S.J. Batista¹⁶⁷, S. Batlamous^{35e}, J.R. Batley³², B. Batool¹⁵¹, M. Battaglia¹⁴⁶, M. Bause^{72a,72b}, F. Bauer¹⁴⁵, K.T. Bauer¹⁷¹, H.S. Bawa^{31,l}, J.B. Beacham⁴⁹, T. Beau¹³⁶, P.H. Beauchemin¹⁷⁰, F. Becherer⁵², P. Bechtel²⁴, H.C. Beck⁵³, H.P. Beck^{20,q}, K. Becker⁵², M. Becker⁹⁹, C. Becot⁴⁶, A. Beddall^{12d}, A.J. Beddall^{12a}, V.A. Bednyakov⁷⁹, M. Bedognetti¹²⁰, C.P. Bee¹⁵⁵, T.A. Beermann⁷⁶, M. Begalli^{80b}, M. Begel²⁹, A. Behera¹⁵⁵, J.K. Behr⁴⁶, F. Beisiegel²⁴, A.S. Bell⁹⁴, G. Bella¹⁶¹, L. Bellagamba^{23b}, A. Bellerive³⁴, P. Bellos⁹, K. Beloborodov^{122b,122a}, K. Belotskiy¹¹², N.L. Belyaev¹¹², O. Benary^{161,*}, D. Benchekroun^{35a}, N. Benekos¹⁰, Y. Benhammou¹⁶¹, D.P. Benjamin⁶, M. Benoit⁵⁴, J.R. Bensinger²⁶, S. Bentvelsen¹²⁰, L. Beresford¹³⁵, M. Beretta⁵¹, D. Berge⁴⁶, E. Bergeas Kuutmann¹⁷², N. Berger⁵, B. Bergmann¹⁴², L.J. Bergsten²⁶, J. Beringer¹⁸, S. Berlendis⁷, N.R. Bernard¹⁰², G. Bernardi¹³⁶, C. Bernius¹⁵³, F.U. Bernlochner²⁴, T. Berry⁹³, P. Berta⁹⁹, C. Bertella^{15a}, I.A. Bertram⁸⁹, G.J. Besjes⁴⁰, O. Bessidskaia Bylund¹⁸², N. Besson¹⁴⁵, A. Bethani¹⁰⁰, S. Bethke¹¹⁵, A. Betti²⁴, A.J. Bevan⁹², J. Beyer¹¹⁵, R. Bi¹³⁹, R.M. Bianchi¹³⁹, O. Biebel¹¹⁴,

D. Biedermann¹⁹, R. Bielski³⁶, K. Bierwagen⁹⁹, N.V. Biesuz^{71a,71b}, M. Biglietti^{74a}, T.R.V. Billoud¹⁰⁹, M. Bindi⁵³, A. Bingul^{12d}, C. Bini^{72a,72b}, S. Biondi^{23b,23a}, M. Birman¹⁸⁰, T. Bisanz⁵³, J.P. Biswal¹⁶¹, A. Bitadze¹⁰⁰, C. Bittrich⁴⁸, D.M. Bjergaard⁴⁹, K. Bjørke¹³⁴, J.E. Black¹⁵³, K.M. Black²⁵, T. Blazek^{28a}, I. Bloch⁴⁶, C. Blocker²⁶, A. Blue⁵⁷, U. Blumenschein⁹², G.J. Bobbink¹²⁰, V.S. Bobrovnikov^{122b,122a}, S.S. Bocchetta⁹⁶, A. Bocci⁴⁹, D. Boerner⁴⁶, D. Bogavac¹⁴, A.G. Bogdanchikov^{122b,122a}, C. Boehm^{45a}, V. Boisvert⁹³, P. Bokan^{53,172}, T. Bold^{83a}, A.S. Boldyrev¹¹³, A.E. Bolz^{61b}, M. Bomben¹³⁶, M. Bona⁹², J.S. Bonilla¹³¹, M. Boonekamp¹⁴⁵, H.M. Borecka-Bielska⁹⁰, A. Borisov¹²³, G. Borissov⁸⁹, J. Bortfeldt³⁶, D. Bortoletto¹³⁵, V. Bortolotto^{73a,73b}, D. Boscherini^{23b}, M. Bosman¹⁴, J.D. Bossio Sola¹⁰³, K. Bouaouda^{35a}, J. Boudreau¹³⁹, E.V. Bouhova-Thacker⁸⁹, D. Boumediene³⁸, S.K. Boutle⁵⁷, A. Boveia¹²⁶, J. Boyd³⁶, D. Boye^{33b,aq}, I.R. Boyko⁷⁹, A.J. Bozson⁹³, J. Bracinik²¹, N. Brahimi¹⁰¹, G. Brandt¹⁸², O. Brandt^{61a}, F. Braren⁴⁶, U. Bratzler¹⁶⁴, B. Brau¹⁰², J.E. Brau¹³¹, W.D. Breaden Madden⁵⁷, K. Brendlinger⁴⁶, L. Brenner⁴⁶, R. Brenner¹⁷², S. Bressler¹⁸⁰, B. Brickwedde⁹⁹, D.L. Briglin²¹, D. Britton⁵⁷, D. Britzger¹¹⁵, I. Brock²⁴, R. Brock¹⁰⁶, G. Brooijmans³⁹, T. Brooks⁹³, W.K. Brooks^{147b}, E. Brost¹²¹, J.H. Broughton²¹, P.A. Bruckman de Renstrom⁸⁴, D. Bruncko^{28b}, A. Bruni^{23b}, G. Bruni^{23b}, L.S. Bruni¹²⁰, S. Bruno^{73a,73b}, B.H. Brunt³², M. Bruschi^{23b}, N. Bruscino¹³⁹, P. Bryant³⁷, L. Bryngemark⁹⁶, T. Buanes¹⁷, Q. Buat³⁶, P. Buchholz¹⁵¹, A.G. Buckley⁵⁷, I.A. Budagov⁷⁹, M.K. Bugge¹³⁴, F. Bühner⁵², O. Bulekov¹¹², T.J. Burch¹²¹, S. Burdin⁹⁰, C.D. Burgard¹²⁰, A.M. Burger¹²⁹, B. Burghgrave⁸, K. Burka⁸⁴, J.T.P. Burr⁴⁶, V. Büscher⁹⁹, E. Buschmann⁵³, P.J. Bussey⁵⁷, J.M. Butler²⁵, C.M. Buttar⁵⁷, J.M. Butterworth⁹⁴, P. Butti³⁶, W. Buttinger³⁶, A. Buzatu¹⁵⁸, A.R. Buzykaev^{122b,122a}, G. Cabras^{23b,23a}, S. Cabrera Urbán¹⁷⁴, D. Caforio⁵⁶, H. Cai¹⁷³, V.M.M. Cairo¹⁵³, O. Cakir^{4a}, N. Calace³⁶, P. Calafiura¹⁸, A. Calandri¹⁰¹, G. Calderini¹³⁶, P. Calfayan⁶⁵, G. Callea⁵⁷, L.P. Caloba^{80b}, S. Calvente Lopez⁹⁸, D. Calvet³⁸, S. Calvet³⁸, T.P. Calvet¹⁵⁵, M. Calvetti^{71a,71b}, R. Camacho Toro¹³⁶, S. Camarda³⁶, D. Camarero Munoz⁹⁸, P. Camarri^{73a,73b}, D. Cameron¹³⁴, R. Caminal Armadans¹⁰², C. Camincher³⁶, S. Campana³⁶, M. Campanelli⁹⁴, A. Camplani⁴⁰, A. Campoverde¹⁵¹, V. Canale^{69a,69b}, A. Canesse¹⁰³, M. Cano Bret^{60c}, J. Cantero¹²⁹, T. Cao¹⁶¹, Y. Cao¹⁷³, M.D.M. Capeans Garrido³⁶, M. Capua^{41b,41a}, R. Cardarelli^{73a}, F.C. Cardillo¹⁴⁹, I. Carli¹⁴³, T. Carli³⁶, G. Carlino^{69a}, B.T. Carlson¹³⁹, L. Carminati^{68a,68b}, R.M.D. Carney^{45a,45b}, S. Caron¹¹⁹, E. Carquin^{147b}, S. Carrá^{68a,68b}, J.W.S. Carter¹⁶⁷, M.P. Casado^{14,e}, A.F. Casha¹⁶⁷, D.W. Casper¹⁷¹, R. Castelijns¹²⁰, F.L. Castillo¹⁷⁴, V. Castillo Gimenez¹⁷⁴, N.F. Castro^{140a,140e}, A. Catinaccio³⁶, J.R. Catmore¹³⁴, A. Cattai³⁶, J. Caudron²⁴, V. Cavaliere²⁹, E. Cavallaro¹⁴, D. Cavalli^{68a}, M. Cavalli-Sforza¹⁴, V. Cavasinni^{71a,71b}, E. Celebi^{12b}, F. Ceradini^{74a,74b}, L. Cerda Alberich¹⁷⁴, A.S. Cerqueira^{80a}, A. Cerri¹⁵⁶, L. Cerrito^{73a,73b}, F. Cerutti¹⁸, A. Cervelli^{23b,23a}, S.A. Cetin^{12b}, A. Chafaq^{35a}, D. Chakraborty¹²¹, S.K. Chan⁵⁹, W.S. Chan¹²⁰, W.Y. Chan⁹⁰, J.D. Chapman³², B. Chargeishvili^{159b}, D.G. Charlton²¹, T.P. Charman⁹², C.C. Chau³⁴, S. Che¹²⁶, A. Chegwidan¹⁰⁶, S. Chekanov⁶, S.V. Chekulaev^{168a}, G.A. Chelkov^{79,av}, M.A. Chelstowska³⁶, B. Chen⁷⁸, C. Chen^{60a}, C.H. Chen⁷⁸, H. Chen²⁹, J. Chen^{60a}, J. Chen³⁹, S. Chen¹³⁷, S.J. Chen^{15c}, X. Chen^{15b,au}, Y. Chen⁸², Y-H. Chen⁴⁶, H.C. Cheng^{63a}, H.J. Cheng^{15a,15d}, A. Cheplakov⁷⁹, E. Cheremushkina¹²³, R. Cherkaoui El Moursli^{35e}, E. Cheu⁷, K. Cheung⁶⁴, T.J.A. Chevaléras¹⁴⁵, L. Chevalier¹⁴⁵, V. Chiarella⁵¹, G. Chiarelli^{71a}, G. Chiodini^{67a}, A.S. Chisholm^{36,21}, A. Chitan^{27b}, I. Chiu¹⁶³, Y.H. Chiu¹⁷⁶, M.V. Chizhov⁷⁹, K. Choi⁶⁵, A.R. Chomont¹³², S. Chouridou¹⁶², Y.S. Chow¹²⁰, M.C. Chu^{63a}, J. Chudoba¹⁴¹, A.J. Chuinard¹⁰³, J.J. Chwastowski⁸⁴, L. Chytka¹³⁰, K.M. Ciesla⁸⁴, D. Cinca⁴⁷, V. Cindro⁹¹, I.A. Cioară^{27b}, A. Ciochio¹⁸, F. Ciotto^{69a,69b}, Z.H. Citron¹⁸⁰, M. Citterio^{68a}, D.A. Ciubotaru^{27b}, B.M. Ciungu¹⁶⁷, A. Clark⁵⁴, M.R. Clark³⁹, P.J. Clark⁵⁰, C. Clement^{45a,45b}, Y. Coadou¹⁰¹, M. Cobal^{66a,66c}, A. Coccaro^{55b}, J. Cochran⁷⁸, H. Cohen¹⁶¹, A.E.C. Coimbra¹⁸⁰, L. Colasurdo¹¹⁹, B. Cole³⁹, A.P. Colijn¹²⁰, J. Collot⁵⁸, P. Conde Muiño^{140a,f}, E. Coniavitis⁵², S.H. Connell^{33b}, I.A. Connelly⁵⁷, S. Constantinescu^{27b}, F. Conventi^{69a,ax}, A.M. Cooper-Sarkar¹³⁵, F. Cormier¹⁷⁵, K.J.R. Cormier¹⁶⁷, L.D. Corpe⁹⁴, M. Corradi^{72a,72b}, E.E. Corrigan⁹⁶, F. Corriveau^{103,ac}, A. Cortes-Gonzalez³⁶, M.J. Costa¹⁷⁴, F. Costanza⁵, D. Costanzo¹⁴⁹, G. Cowan⁹³, J.W. Cowley³², J. Crane¹⁰⁰, K. Cranmer¹²⁴, S.J. Crawley⁵⁷, R.A. Creager¹³⁷, S. Crépe-Renaudin⁵⁸, F. Crescioli¹³⁶, M. Cristinziani²⁴, V. Croft¹²⁰, G. Crosetti^{41b,41a}, A. Cueto⁵, T. Cuhadar Donszelmann¹⁴⁹, A.R. Cukierman¹⁵³, S. Czekierda⁸⁴, P. Czodrowski³⁶, M.J. Da Cunha Sargedas De Sousa^{60b}, J.V. Da Fonseca Pinto^{80b}, C. Da Via¹⁰⁰, W. Dabrowski^{83a}, T. Dado^{28a}, S. Dahbi^{35e}, T. Dai¹⁰⁵, C. Dallapiccola¹⁰², M. Dam⁴⁰, G. D'amen^{23b,23a}, V. D'Amico^{74a,74b}, J. Damp⁹⁹, J.R. Dandoy¹³⁷, M.F. Daneri³⁰, N.P. Dang¹⁸¹, N.D. Dann¹⁰⁰, M. Danninger¹⁷⁵, V. Dao³⁶,

G. Darbo^{55b}, O. Dartsis⁵, A. Dattagupta¹³¹, T. Daubney⁴⁶, S. D'Auria^{68a,68b}, W. Davey²⁴, C. David⁴⁶, T. Davidek¹⁴³, D.R. Davis⁴⁹, E. Dawe¹⁰⁴, I. Dawson¹⁴⁹, K. De⁸, R. De Asmundis^{69a}, A. De Benedetti¹²⁸, M. De Beurs¹²⁰, S. De Castro^{23b,23a}, S. De Cecco^{72a,72b}, N. De Groot¹¹⁹, P. de Jong¹²⁰, H. De la Torre¹⁰⁶, A. De Maria^{15c}, D. De Pedis^{72a}, A. De Salvo^{72a}, U. De Sanctis^{73a,73b}, M. De Santis^{73a,73b}, A. De Santo¹⁵⁶, K. De Vasconcelos Corga¹⁰¹, J.B. De Vivie De Regie¹³², C. Debenedetti¹⁴⁶, D.V. Dedovich⁷⁹, A.M. Deiana⁴², M. Del Gaudio^{41b,41a}, J. Del Peso⁹⁸, Y. Delabat Diaz⁴⁶, D. Delgove¹³², F. Deliot¹⁴⁵, C.M. Delitzsch⁷, M. Della Pietra^{69a,69b}, D. Della Volpe⁵⁴, A. Dell'Acqua³⁶, L. Dell'Asta²⁵, M. Delmastro⁵, C. Delponte¹³², P.A. Delsart⁵⁸, D.A. DeMarco¹⁶⁷, S. Demers¹⁸³, M. Demichev⁷⁹, G. Demontigny¹⁰⁹, S.P. Denisov¹²³, D. Denysiuk¹²⁰, L. D'Eramo¹³⁶, D. Derendarz⁸⁴, J.E. Derkaoui^{35d}, F. Derue¹³⁶, P. Dervan⁹⁰, K. Desch²⁴, C. Deterre⁴⁶, K. Dette¹⁶⁷, M.R. Devesa³⁰, P.O. Deviveiros³⁶, A. Dewhurst¹⁴⁴, S. Dhaliwal²⁶, F.A. Di Bello⁵⁴, A. Di Ciaccio^{73a,73b}, L. Di Ciaccio⁵, W.K. Di Clemente¹³⁷, C. Di Donato^{69a,69b}, A. Di Girolamo³⁶, G. Di Gregorio^{71a,71b}, B. Di Micco^{74a,74b}, R. Di Nardo¹⁰², K.F. Di Petrillo⁵⁹, R. Di Sipio¹⁶⁷, D. Di Valentino³⁴, C. Diaconu¹⁰¹, F.A. Dias⁴⁰, T. Dias Do Vale^{140a,140e}, M.A. Diaz^{147a}, J. Dickinson¹⁸, E.B. Diehl¹⁰⁵, J. Dietrich¹⁹, S. Díez Cornell⁴⁶, A. Dimitrievska¹⁸, W. Ding^{15b}, J. Dingfelder²⁴, F. Dittus³⁶, F. Djama¹⁰¹, T. Djobava^{159b}, J.I. Djuvsland¹⁷, M.A.B. Do Vale^{80c}, M. Dobre^{27b}, D. Dodsworth²⁶, C. Doglioni⁹⁶, J. Dolejsi¹⁴³, Z. Dolezal¹⁴³, M. Donadelli^{80d}, J. Donini³⁸, A. D'onofrio⁹², M. D'Onofrio⁹⁰, J. Dopke¹⁴⁴, A. Doria^{69a}, M.T. Dova⁸⁸, A.T. Doyle⁵⁷, E. Drechsler¹⁵², E. Dreyer¹⁵², T. Dreyer⁵³, Y. Du^{60b}, Y. Duan^{60b}, F. Dubinin¹¹⁰, M. Dubovsky^{28a}, A. Dubreuil⁵⁴, E. Duchovni¹⁸⁰, G. Duckeck¹¹⁴, A. Ducourthial¹³⁶, O.A. Ducu¹⁰⁹, D. Duda¹¹⁵, A. Dudarev³⁶, A.C. Dudder⁹⁹, E.M. Duffield¹⁸, L. Dufлот¹³², M. Dührssen³⁶, C. Dülsen¹⁸², M. Dumancic¹⁸⁰, A.E. Dumitriu^{27b}, A.K. Duncan⁵⁷, M. Dunford^{61a}, A. Duperrin¹⁰¹, H. Duran Yildiz^{4a}, M. Düren⁵⁶, A. Durglishvili^{159b}, D. Duschinger⁴⁸, B. Dutta⁴⁶, D. Duvnjak¹, G.I. Dyckes¹³⁷, M. Dyndal³⁶, S. Dysch¹⁰⁰, B.S. Dziedzic⁸⁴, K.M. Ecker¹¹⁵, R.C. Edgar¹⁰⁵, T. Eifert³⁶, G. Eigen¹⁷, K. Einsweiler¹⁸, T. Ekelof¹⁷², M. El Kacimi^{35c}, R. El Kosseifi¹⁰¹, V. Ellajosyula¹⁷², M. Ellert¹⁷², F. Ellinghaus¹⁸², A.A. Elliot⁹², N. Ellis³⁶, J. Elmsheuser²⁹, M. Elsing³⁶, D. Emelianov¹⁴⁴, A. Emerman³⁹, Y. Enari¹⁶³, J.S. Ennis¹⁷⁸, M.B. Epland⁴⁹, J. Erdmann⁴⁷, A. Ereditato²⁰, M. Escalier¹³², C. Escobar¹⁷⁴, O. Estrada Pastor¹⁷⁴, A.I. Etienvre¹⁴⁵, E. Etzion¹⁶¹, H. Evans⁶⁵, A. Ezhilov¹³⁸, F. Fabbri⁵⁷, L. Fabbri^{23b,23a}, V. Fabiani¹¹⁹, G. Facini⁹⁴, R.M. Faisca Rodrigues Pereira^{140a}, R.M. Fakhrutdinov¹²³, S. Falciano^{72a}, P.J. Falke⁵, S. Falke⁵, J. Faltova¹⁴³, Y. Fang^{15a}, Y. Fang^{15a}, G. Fanourakis⁴⁴, M. Fanti^{68a,68b}, A. Farbin⁸, A. Farilla^{74a}, E.M. Farina^{70a,70b}, T. Farooque¹⁰⁶, S. Farrell¹⁸, S.M. Farrington¹⁷⁸, P. Farthouat³⁶, F. Fassi^{35e}, P. Fassnacht³⁶, D. Fassouliotis⁹, M. Fauci Giannelli⁵⁰, W.J. Fawcett³², L. Fayard¹³², O.L. Fedin^{138,o}, W. Fedorko¹⁷⁵, M. Feickert⁴², S. Feigl¹³⁴, L. Feligioni¹⁰¹, A. Fell¹⁴⁹, C. Feng^{60b}, E.J. Feng³⁶, M. Feng⁴⁹, M.J. Fenton⁵⁷, A.B. Fenyuk¹²³, J. Ferrando⁴⁶, A. Ferrante¹⁷³, A. Ferrari¹⁷², P. Ferrari¹²⁰, R. Ferrari^{70a}, D.E. Ferreira de Lima^{61b}, A. Ferrer¹⁷⁴, D. Ferrere⁵⁴, C. Ferretti¹⁰⁵, F. Fiedler⁹⁹, A. Filipčič⁹¹, F. Filthaut¹¹⁹, K.D. Finelli²⁵, M.C.N. Fiolhais^{140a}, L. Fiorini¹⁷⁴, F. Fischer¹¹⁴, W.C. Fisher¹⁰⁶, I. Fleck¹⁵¹, P. Fleischmann¹⁰⁵, R.R.M. Fletcher¹³⁷, T. Flick¹⁸², B.M. Flierl¹¹⁴, L.F. Flores¹³⁷, L.R. Flores Castillo^{63a}, F.M. Follega^{75a,75b}, N. Fomin¹⁷, G.T. Forcolin^{75a,75b}, A. Formica¹⁴⁵, F.A. Förster¹⁴, A.C. Forti¹⁰⁰, A.G. Foster²¹, M.G. Foti¹³⁵, D. Fournier¹³², H. Fox⁸⁹, S. Fracchia¹⁴⁹, P. Francavilla^{71a,71b}, M. Franchini^{23b,23a}, S. Franchino^{61a}, D. Francis³⁶, L. Franconi²⁰, M. Franklin⁵⁹, M. Frate¹⁷¹, A.N. Fray⁹², B. Freund¹⁰⁹, W.S. Freund^{80b}, E.M. Freundlich⁴⁷, D.C. Frizzell¹²⁸, D. Froidevaux³⁶, J.A. Frost¹³⁵, C. Fukunaga¹⁶⁴, E. Fullana Torregrosa¹⁷⁴, E. Fumagalli^{55b,55a}, T. Fusayasu¹¹⁶, J. Fuster¹⁷⁴, A. Gabrielli^{23b,23a}, A. Gabrielli¹⁸, G.P. Gach^{83a}, S. Gadatsch⁵⁴, P. Gadow¹¹⁵, G. Gagliardi^{55b,55a}, L.G. Gagnon¹⁰⁹, C. Galea^{27b}, B. Galhardo^{140a,140c}, G.E. Gallardo¹³⁵, E.J. Gallas¹³⁵, B.J. Gallop¹⁴⁴, P. Gallus¹⁴², G. Galster⁴⁰, R. Gamboa Goni⁹², K.K. Gan¹²⁶, S. Ganguly¹⁸⁰, J. Gao^{60a}, Y. Gao⁹⁰, Y.S. Gao^{31,l}, C. García¹⁷⁴, J.E. García Navarro¹⁷⁴, J.A. García Pascual^{15a}, C. Garcia-Argos⁵², M. Garcia-Sciveres¹⁸, R.W. Gardner³⁷, N. Garelli¹⁵³, S. Gargiulo⁵², V. Garonne¹³⁴, A. Gaudiello^{55b,55a}, G. Gaudio^{70a}, I.L. Gavrilenko¹¹⁰, A. Gavrilyuk¹¹¹, C. Gay¹⁷⁵, G. Gaycken²⁴, E.N. Gazis¹⁰, A.A. Geanta^{27b}, C.N.P. Gee¹⁴⁴, J. Geisen⁵³, M. Geisen⁹⁹, M.P. Geisler^{61a}, C. Gemme^{55b}, M.H. Genest⁵⁸, C. Geng¹⁰⁵, S. Gentile^{72a,72b}, S. George⁹³, T. Gerialis⁴⁴, D. Gerbaudo¹⁴, L.O. Gerlach⁵³, P. Gessinger-Befurt⁹⁹, G. Gessner⁴⁷, S. Ghasemi¹⁵¹, M. Ghasemi Bostanabad¹⁷⁶, M. Ghneimat²⁴, A. Ghosh⁷⁷, B. Giacobbe^{23b}, S. Giagu^{72a,72b}, N. Giangiacomi^{23b,23a}, P. Giannetti^{71a}, A. Giannini^{69a,69b}, S.M. Gibson⁹³, M. Gignac¹⁴⁶, D. Gillberg³⁴, G. Gilles¹⁸², D.M. Gingrich^{3,aw}, M.P. Giordani^{66a,66c}, F.M. Giorgi^{23b}, P.F. Giraud¹⁴⁵,

G. Giugliarelli ^{66a,66c}, D. Giugni ^{68a}, F. Giuli ^{73a,73b}, M. Giulini ^{61b}, S. Gkaitatzis ¹⁶², I. Gkialas ^{9,h}, E.L. Gkougkousis ¹⁴, P. Gkoutoumis ¹⁰, L.K. Gladilin ¹¹³, C. Glasman ⁹⁸, J. Glatzer ¹⁴, P.C.F. Glaysheer ⁴⁶, A. Glazov ⁴⁶, M. Goblirsch-Kolb ²⁶, S. Goldfarb ¹⁰⁴, T. Golling ⁵⁴, D. Golubkov ¹²³, A. Gomes ^{140a,140b}, R. Goncalves Gama ⁵³, R. Gonçalves ^{140a,140b}, G. Gonella ⁵², L. Gonella ²¹, A. Gongadze ⁷⁹, F. Gonnella ²¹, J.L. Gonski ⁵⁹, S. González de la Hoz ¹⁷⁴, S. Gonzalez-Sevilla ⁵⁴, G.R. Gonzalvo Rodriguez ¹⁷⁴, L. Goossens ³⁶, P.A. Gorbounov ¹¹¹, H.A. Gordon ²⁹, B. Gorini ³⁶, E. Gorini ^{67a,67b}, A. Gorišek ⁹¹, A.T. Goshaw ⁴⁹, C. Gössling ⁴⁷, M.I. Gostkin ⁷⁹, C.A. Gottardo ²⁴, C.R. Goudet ¹³², M. Gouighri ^{35b}, D. Goujdami ^{35c}, A.G. Goussiou ¹⁴⁸, N. Govender ^{33b,a}, C. Goy ⁵, E. Gozani ¹⁶⁰, I. Grabowska-Bold ^{83a}, P.O.J. Gradin ¹⁷², E.C. Graham ⁹⁰, J. Gramling ¹⁷¹, E. Gramstad ¹³⁴, S. Grancagnolo ¹⁹, M. Grandi ¹⁵⁶, V. Gratchev ¹³⁸, P.M. Gravila ^{27f}, F.G. Gravili ^{67a,67b}, C. Gray ⁵⁷, H.M. Gray ¹⁸, C. Grefe ²⁴, K. Gregersen ⁹⁶, I.M. Gregor ⁴⁶, P. Grenier ¹⁵³, K. Grevtsov ⁴⁶, N.A. Grieser ¹²⁸, J. Griffiths ⁸, A.A. Grillo ¹⁴⁶, K. Grimm ^{31,k}, S. Grinstein ^{14,w}, J.-F. Grivaz ¹³², S. Groh ⁹⁹, E. Gross ¹⁸⁰, J. Grosse-Knetter ⁵³, Z.J. Grout ⁹⁴, C. Grud ¹⁰⁵, A. Grummer ¹¹⁸, L. Guan ¹⁰⁵, W. Guan ¹⁸¹, J. Guenther ³⁶, A. Guerguichon ¹³², F. Guescini ^{168a}, D. Guest ¹⁷¹, R. Gugel ⁵², B. Gui ¹²⁶, T. Guillemain ⁵, S. Guindon ³⁶, U. Gul ⁵⁷, J. Guo ^{60c}, W. Guo ¹⁰⁵, Y. Guo ^{60a,r}, Z. Guo ¹⁰¹, R. Gupta ⁴⁶, S. Gurbuz ^{12c}, G. Gustavino ¹²⁸, P. Gutierrez ¹²⁸, C. Gutsche ⁹⁴, C. Guyot ¹⁴⁵, M.P. Guzik ^{83a}, C. Gwenlan ¹³⁵, C.B. Gwilliam ⁹⁰, A. Haas ¹²⁴, C. Haber ¹⁸, H.K. Hadavand ⁸, N. Haddad ^{35e}, A. Hadeef ^{60a}, S. Hageböck ³⁶, M. Hagihara ¹⁶⁹, M. Haleem ¹⁷⁷, J. Haley ¹²⁹, G. Halladjian ¹⁰⁶, G.D. Hallewell ¹⁰¹, K. Hamacher ¹⁸², P. Hamal ¹³⁰, K. Hamano ¹⁷⁶, H. Hamdaoui ^{35e}, G.N. Hamity ¹⁴⁹, K. Han ^{60a,qj}, L. Han ^{60a}, S. Han ^{15a,15d}, K. Hanagaki ^{81,u}, M. Hance ¹⁴⁶, D.M. Handl ¹¹⁴, B. Haney ¹³⁷, R. Hankache ¹³⁶, P. Hanke ^{61a}, E. Hansen ⁹⁶, J.B. Hansen ⁴⁰, J.D. Hansen ⁴⁰, M.C. Hansen ²⁴, P.H. Hansen ⁴⁰, E.C. Hanson ¹⁰⁰, K. Hara ¹⁶⁹, A.S. Hard ¹⁸¹, T. Harenberg ¹⁸², S. Harkusha ¹⁰⁷, P.F. Harrison ¹⁷⁸, N.M. Hartmann ¹¹⁴, Y. Hasegawa ¹⁵⁰, A. Hasib ⁵⁰, S. Hassani ¹⁴⁵, S. Haug ²⁰, R. Hauser ¹⁰⁶, L. Hauswald ⁴⁸, L.B. Havener ³⁹, M. Havranek ¹⁴², C.M. Hawkes ²¹, R.J. Hawkins ³⁶, D. Hayden ¹⁰⁶, C. Hayes ¹⁵⁵, R.L. Hayes ¹⁷⁵, C.P. Hays ¹³⁵, J.M. Hays ⁹², H.S. Hayward ⁹⁰, S.J. Haywood ¹⁴⁴, F. He ^{60a}, M.P. Heath ⁵⁰, V. Hedberg ⁹⁶, L. Heelan ⁸, S. Heer ²⁴, K.K. Heidegger ⁵², J. Heilman ³⁴, S. Heim ⁴⁶, T. Heim ¹⁸, B. Heinemann ^{46,ar}, J.J. Heinrich ¹³¹, L. Heinrich ³⁶, C. Heinz ⁵⁶, J. Hejbal ¹⁴¹, L. Helary ^{61b}, A. Held ¹⁷⁵, S. Hellesund ¹³⁴, C.M. Helling ¹⁴⁶, S. Hellman ^{45a,45b}, C. Helsens ³⁶, R.C.W. Henderson ⁸⁹, Y. Heng ¹⁸¹, S. Henkelmann ¹⁷⁵, A.M. Henriques Correia ³⁶, G.H. Herbert ¹⁹, H. Herde ²⁶, V. Herget ¹⁷⁷, Y. Hernández Jiménez ^{33c}, H. Herr ⁹⁹, M.G. Herrmann ¹¹⁴, T. Herrmann ⁴⁸, G. Herten ⁵², R. Hertenberger ¹¹⁴, L. Hervas ³⁶, T.C. Herwig ¹³⁷, G.G. Hesketh ⁹⁴, N.P. Hessey ^{168a}, A. Higashida ¹⁶³, S. Higashino ⁸¹, E. Higón-Rodríguez ¹⁷⁴, K. Hildebrand ³⁷, E. Hill ¹⁷⁶, J.C. Hill ³², K.K. Hill ²⁹, K.H. Hiller ⁴⁶, S.J. Hillier ²¹, M. Hils ⁴⁸, I. Hinchliffe ¹⁸, F. Hinterkeuser ²⁴, M. Hirose ¹³³, S. Hirose ⁵², D. Hirschbuehl ¹⁸², B. Hiti ⁹¹, O. Hladik ¹⁴¹, D.R. Hlaluku ^{33c}, X. Hoad ⁵⁰, J. Hobbs ¹⁵⁵, N. Hod ¹⁸⁰, M.C. Hodgkinson ¹⁴⁹, A. Hoecker ³⁶, F. Hoenig ¹¹⁴, D. Hohn ⁵², D. Hohov ¹³², T.R. Holmes ³⁷, M. Holzbock ¹¹⁴, L.B.A.H. Hommels ³², S. Honda ¹⁶⁹, T. Honda ⁸¹, T.M. Hong ¹³⁹, A. Hönle ¹¹⁵, B.H. Hooberman ¹⁷³, W.H. Hopkins ⁶, Y. Horii ¹¹⁷, P. Horn ⁴⁸, A.J. Horton ¹⁵², L.A. Horyn ³⁷, J.-Y. Hostachy ⁵⁸, A. Hostiuc ¹⁴⁸, S. Hou ¹⁵⁸, A. Hoummada ^{35a}, J. Howarth ¹⁰⁰, J. Hoya ⁸⁸, M. Hrabovsky ¹³⁰, J. Hrdinka ⁷⁶, I. Hristova ¹⁹, J. Hrivnac ¹³², A. Hrynevich ¹⁰⁸, T. Hryn'ova ⁵, P.J. Hsu ⁶⁴, S.-C. Hsu ¹⁴⁸, Q. Hu ²⁹, S. Hu ^{60c}, Y. Huang ^{15a}, Z. Hubacek ¹⁴², F. Hubaut ¹⁰¹, M. Huebner ²⁴, F. Huegging ²⁴, T.B. Huffman ¹³⁵, M. Huhtinen ³⁶, R.F.H. Hunter ³⁴, P. Huo ¹⁵⁵, A.M. Hupe ³⁴, N. Huseynov ^{79,ae}, J. Huston ¹⁰⁶, J. Huth ⁵⁹, R. Hyneman ¹⁰⁵, S. Hyrych ^{28a}, G. Iacobucci ⁵⁴, G. Iakovidis ²⁹, I. Ibragimov ¹⁵¹, L. Iconomidou-Fayard ¹³², Z. Idrissi ^{35e}, P.I. Iengo ³⁶, R. Ignazzi ⁴⁰, O. Igonkina ^{120,y}, R. Iguchi ¹⁶³, T. Iizawa ⁵⁴, Y. Ikegami ⁸¹, M. Ikeno ⁸¹, D. Iliadis ¹⁶², N. Ilic ¹¹⁹, F. Iltzsche ⁴⁸, G. Introzzi ^{70a,70b}, M. Iodice ^{74a}, K. Iordanidou ³⁹, V. Ippolito ^{72a,72b}, M.F. Isacson ¹⁷², N. Ishijima ¹³³, M. Ishino ¹⁶³, M. Ishitsuka ¹⁶⁵, W. Islam ¹²⁹, C. Issever ¹³⁵, S. Istin ¹⁶⁰, F. Ito ¹⁶⁹, J.M. Iturbe Ponce ^{63a}, R. Iuppa ^{75a,75b}, A. Ivina ¹⁸⁰, H. Iwasaki ⁸¹, J.M. Izen ⁴³, V. Izzo ^{69a}, P. Jacka ¹⁴¹, P. Jackson ¹, R.M. Jacobs ²⁴, V. Jain ², G. Jäkel ¹⁸², K.B. Jakobi ⁹⁹, K. Jakobs ⁵², S. Jakobsen ⁷⁶, T. Jakoubek ¹⁴¹, J. Jamieson ⁵⁷, R. Jansky ⁵⁴, J. Janssen ²⁴, M. Janus ⁵³, P.A. Janus ^{83a}, G. Jarlskog ⁹⁶, N. Javadov ^{79,ae}, T. Javůrek ³⁶, M. Javurkova ⁵², F. Jeanneau ¹⁴⁵, L. Jeanty ¹³¹, J. Jejelava ^{159a,af}, A. Jelinskas ¹⁷⁸, P. Jenni ^{52,b}, J. Jeong ⁴⁶, N. Jeong ⁴⁶, S. Jézéquel ⁵, H. Ji ¹⁸¹, J. Jia ¹⁵⁵, H. Jiang ⁷⁸, Y. Jiang ^{60a}, Z. Jiang ^{153,p}, S. Jiggins ⁵², F.A. Jimenez Morales ³⁸, J. Jimenez Pena ¹⁷⁴, S. Jin ^{15c}, A. Jinaru ^{27b}, O. Jinnouchi ¹⁶⁵, H. Jivan ^{33c}, P. Johansson ¹⁴⁹, K.A. Johns ⁷, C.A. Johnson ⁶⁵, K. Jon-And ^{45a,45b}, R.W.L. Jones ⁸⁹, S.D. Jones ¹⁵⁶, S. Jones ⁷, T.J. Jones ⁹⁰, J. Jongmanns ^{61a}, P.M. Jorge ^{140a,140b}, J. Jovicevic ³⁶,

X. Ju¹⁸, J.J. Junggeburth¹¹⁵, A. Juste Rozas^{14,w}, A. Kaczmarska⁸⁴, M. Kado¹³², H. Kagan¹²⁶, M. Kagan¹⁵³, T. Kaji¹⁷⁹, E. Kajomovitz¹⁶⁰, C.W. Kalderon⁹⁶, A. Kaluza⁹⁹, A. Kamenshchikov¹²³, L. Kanjir⁹¹, Y. Kano¹⁶³, V.A. Kantserov¹¹², J. Kanzaki⁸¹, L.S. Kaplan¹⁸¹, D. Kar^{33c}, M.J. Kareem^{168b}, E. Karentzos¹⁰, S.N. Karpov⁷⁹, Z.M. Karpova⁷⁹, V. Kartvelishvili⁸⁹, A.N. Karyukhin¹²³, L. Kashif¹⁸¹, R.D. Kass¹²⁶, A. Kastanas^{45a,45b}, Y. Kataoka¹⁶³, C. Kato^{60d,60c}, J. Katzy⁴⁶, K. Kawade⁸², K. Kawagoe⁸⁷, T. Kawaguchi¹¹⁷, T. Kawamoto¹⁶³, G. Kawamura⁵³, E.F. Kay¹⁷⁶, V.F. Kazanin^{122b,122a}, R. Keeler¹⁷⁶, R. Kehoe⁴², J.S. Keller³⁴, E. Kellermann⁹⁶, D. Kelsey¹⁵⁶, J.J. Kempster²¹, J. Kendrick²¹, O. Kepka¹⁴¹, S. Kersten¹⁸², B.P. Kerševan⁹¹, S. Ketabchi Haghighat¹⁶⁷, R.A. Keyes¹⁰³, M. Khader¹⁷³, F. Khalil-Zada¹³, M.K. Khandoga¹⁴⁵, A. Khanov¹²⁹, A.G. Kharlamov^{122b,122a}, T. Kharlamova^{122b,122a}, E.E. Khoda¹⁷⁵, A. Khodinov¹⁶⁶, T.J. Khoo⁵⁴, E. Khramov⁷⁹, J. Khubua^{159b}, S. Kido⁸², M. Kiehn⁵⁴, C.R. Kilby⁹³, Y.K. Kim³⁷, N. Kimura^{66a,66c}, O.M. Kind¹⁹, B.T. King^{90,*}, D. Kirchmeier⁴⁸, J. Kirk¹⁴⁴, A.E. Kiryunin¹¹⁵, T. Kishimoto¹⁶³, D.P. Kisliuk¹⁶⁷, V. Kitali⁴⁶, O. Kivernyk⁵, E. Kladiwa^{28b,*}, T. Klapdor-Kleingrothaus⁵², M.H. Klein¹⁰⁵, M. Klein⁹⁰, U. Klein⁹⁰, K. Kleinknecht⁹⁹, P. Klimek¹²¹, A. Klimentov²⁹, T. Klingl²⁴, T. Klioutchnikova³⁶, F.F. Klitzner¹¹⁴, P. Kluit¹²⁰, S. Kluth¹¹⁵, E. Kneringer⁷⁶, E.B.F.G. Knoops¹⁰¹, A. Knue⁵², D. Kobayashi⁸⁷, T. Kobayashi¹⁶³, M. Kobel⁴⁸, M. Kocian¹⁵³, P. Kodys¹⁴³, P.T. Koenig²⁴, T. Koffas³⁴, N.M. Köhler¹¹⁵, T. Koi¹⁵³, M. Kolb^{61b}, I. Koletsou⁵, T. Komarek¹³⁰, T. Kondo⁸¹, N. Kondrashova^{60c}, K. Köneke⁵², A.C. König¹¹⁹, T. Kono¹²⁵, R. Konoplich^{124,am}, V. Konstantinides⁹⁴, N. Konstantinidis⁹⁴, B. Konya⁹⁶, R. Kopeliansky⁶⁵, S. Koperny^{83a}, K. Korcyl⁸⁴, K. Kordas¹⁶², G. Koren¹⁶¹, A. Korn⁹⁴, I. Korolkov¹⁴, E.V. Korolkova¹⁴⁹, N. Korotkova¹¹³, O. Kortner¹¹⁵, S. Kortner¹¹⁵, T. Kosek¹⁴³, V.V. Kostyukhin²⁴, A. Kotwal⁴⁹, A. Koulouris¹⁰, A. Kourkoumeli-Charalampidi^{70a,70b}, C. Kourkoumelis⁹, E. Kourlitis¹⁴⁹, V. Kouskoura²⁹, A.B. Kowalewska⁸⁴, R. Kowalewski¹⁷⁶, C. Kozakai¹⁶³, W. Kozanecki¹⁴⁵, A.S. Kozhin¹²³, V.A. Kramarenko¹¹³, G. Kramberger⁹¹, D. Krasnopevtsev^{60a}, M.W. Krasny¹³⁶, A. Krasznahorkay³⁶, D. Krauss¹¹⁵, J.A. Kremer^{83a}, J. Kretzschmar⁹⁰, P. Krieger¹⁶⁷, F. Krieter¹¹⁴, A. Krishnan^{61b}, K. Krizka¹⁸, K. Kroeninger⁴⁷, H. Kroha¹¹⁵, J. Kroll¹⁴¹, J. Kroll¹³⁷, J. Krstic¹⁶, U. Kruchonak⁷⁹, H. Krüger²⁴, N. Krumnack⁷⁸, M.C. Kruse⁴⁹, T. Kubota¹⁰⁴, S. Kuday^{4b}, J.T. Kuechler⁴⁶, S. Kuehn³⁶, A. Kugel^{61a}, T. Kuhl⁴⁶, V. Kukhtin⁷⁹, R. Kukla¹⁰¹, Y. Kulchitsky^{107,ai}, S. Kuleshov^{147b}, Y.P. Kulinich¹⁷³, M. Kuna⁵⁸, T. Kunigo⁸⁵, A. Kupco¹⁴¹, T. Kupfer⁴⁷, O. Kuprash⁵², H. Kurashige⁸², L.L. Kurchaninov^{168a}, Y.A. Kurochkin¹⁰⁷, A. Kurova¹¹², M.G. Kurth^{15a,15d}, E.S. Kuwertz³⁶, M. Kuze¹⁶⁵, A.K. Kvam¹⁴⁸, J. Kvita¹³⁰, T. Kwan¹⁰³, A. La Rosa¹¹⁵, J.L. La Rosa Navarro^{80d}, L. La Rotonda^{41b,41a}, F. La Ruffa^{41b,41a}, C. Lacasta¹⁷⁴, F. Lacava^{72a,72b}, D.P.J. Lack¹⁰⁰, H. Lacker¹⁹, D. Lacour¹³⁶, E. Ladygin⁷⁹, R. Lafaye⁵, B. Laforge¹³⁶, T. Lagouri^{33c}, S. Lai⁵³, S. Lammers⁶⁵, W. Lampl⁷, E. Lançon²⁹, U. Landgraf⁵², M.P.J. Landon⁹², M.C. Lanfermann⁵⁴, V.S. Lang⁴⁶, J.C. Lange⁵³, R.J. Langenberg³⁶, A.J. Lankford¹⁷¹, F. Lanni²⁹, K. Lantzsch²⁴, A. Lanza^{70a}, A. Lapertosa^{55b,55a}, S. Laplace¹³⁶, J.F. Laporte¹⁴⁵, T. Lari^{68a}, F. Lasagni Manghi^{23b,23a}, M. Lassnig³⁶, T.S. Lau^{63a}, A. Laudrain¹³², A. Laurier³⁴, M. Lavorgna^{69a,69b}, M. Lazzaroni^{68a,68b}, B. Le¹⁰⁴, O. Le Dortz¹³⁶, E. Le Guirriec¹⁰¹, M. LeBlanc⁷, T. LeCompte⁶, F. Ledroit-Guillon⁵⁸, C.A. Lee²⁹, G.R. Lee¹⁷, L. Lee⁵⁹, S.C. Lee¹⁵⁸, S.J. Lee³⁴, B. Lefebvre^{168a}, M. Lefebvre¹⁷⁶, F. Legger¹¹⁴, C. Leggett¹⁸, K. Lehmann¹⁵², N. Lehmann¹⁸², G. Lehmann Miotto³⁶, W.A. Leight⁴⁶, A. Leisos^{162,v}, M.A.L. Leite^{80d}, R. Leitner¹⁴³, D. Lellouch^{180,*}, K.J.C. Leney⁴², T. Lenz²⁴, B. Lenzi³⁶, R. Leone⁷, S. Leone^{71a}, C. Leonidopoulos⁵⁰, A. Leopold¹³⁶, G. Lerner¹⁵⁶, C. Leroy¹⁰⁹, R. Les¹⁶⁷, C.G. Lester³², M. Levchenko¹³⁸, J. Levêque⁵, D. Levin¹⁰⁵, L.J. Levinson¹⁸⁰, D.J. Lewis²¹, B. Li^{15b}, B. Li¹⁰⁵, C-Q. Li^{60a}, F. Li^{60c}, H. Li^{60a}, H. Li^{60b}, J. Li^{60c}, K. Li¹⁵³, L. Li^{60c}, M. Li^{15a}, Q. Li^{15a,15d}, Q.Y. Li^{60a}, S. Li^{60d,60c}, X. Li⁴⁶, Y. Li⁴⁶, Z. Li^{60b}, Z. Liang^{15a}, B. Liberti^{73a}, A. Liblong¹⁶⁷, K. Lie^{63c}, S. Liem¹²⁰, C.Y. Lin³², K. Lin¹⁰⁶, T.H. Lin⁹⁹, R.A. Linck⁶⁵, J.H. Lindon²¹, A.L. Lioni⁵⁴, E. Lipeles¹³⁷, A. Lipniacka¹⁷, M. Lisovsky^{61b}, T.M. Liss^{173,at}, A. Lister¹⁷⁵, A.M. Litke¹⁴⁶, J.D. Little⁸, B. Liu^{78,ab}, B.L. Liu⁶, H.B. Liu²⁹, H. Liu¹⁰⁵, J.B. Liu^{60a}, J.K.K. Liu¹³⁵, K. Liu¹³⁶, M. Liu^{60a}, P. Liu¹⁸, Y. Liu^{15a,15d}, Y.L. Liu¹⁰⁵, Y.W. Liu^{60a}, M. Livan^{70a,70b}, A. Lleres⁵⁸, J. Llorente Merino^{15a}, S.L. Lloyd⁹², C.Y. Lo^{63b}, F. Lo Sterzo⁴², E.M. Lobodzinska⁴⁶, P. Loch⁷, S. Loffredo^{73a,73b}, T. Lohse¹⁹, K. Lohwasser¹⁴⁹, M. Lokajicek¹⁴¹, J.D. Long¹⁷³, R.E. Long⁸⁹, L. Longo³⁶, K.A. Looper¹²⁶, J.A. Lopez^{147b}, I. Lopez Paz¹⁰⁰, A. Lopez Solis¹⁴⁹, J. Lorenz¹¹⁴, N. Lorenzo Martinez⁵, M. Losada²², P.J. Lösel¹¹⁴, A. Lösle⁵², X. Lou⁴⁶, X. Lou^{15a}, A. Lounis¹³², J. Love⁶, P.A. Love⁸⁹, J.J. Lozano Bahilo¹⁷⁴, H. Lu^{63a}, M. Lu^{60a}, Y.J. Lu⁶⁴, H.J. Lubatti¹⁴⁸, C. Luci^{72a,72b}, A. Lucotte⁵⁸, C. Luedtke⁵², F. Luehring⁶⁵, I. Luise¹³⁶, L. Luminari^{72a}, B. Lund-Jensen¹⁵⁴, M.S. Lutz¹⁰², D. Lynn²⁹, R. Lysak¹⁴¹, E. Lytken⁹⁶, F. Lyu^{15a}, V. Lyubushkin⁷⁹, T. Lyubushkina⁷⁹, H. Ma²⁹,

L.L. Ma^{60b}, Y. Ma^{60b}, G. Maccarrone⁵¹, A. Macchiolo¹¹⁵, C.M. Macdonald¹⁴⁹, J. Machado Miguens¹³⁷, D. Madaffari¹⁷⁴, R. Madar³⁸, W.F. Mader⁴⁸, N. Madysa⁴⁸, J. Maeda⁸², K. Maekawa¹⁶³, S. Maeland¹⁷, T. Maeno²⁹, M. Maerker⁴⁸, A.S. Maevskiy¹¹³, V. Magerl⁵², N. Magini⁷⁸, D.J. Mahon³⁹, C. Maidantchik^{80b}, T. Maier¹¹⁴, A. Maio^{140a,140b,140d}, O. Majersky^{28a}, S. Majewski¹³¹, Y. Makida⁸¹, N. Makovec¹³², B. Malaescu¹³⁶, Pa. Malecki⁸⁴, V.P. Maleev¹³⁸, F. Malek⁵⁸, U. Mallik⁷⁷, D. Malon⁶, C. Malone³², S. Maltezos¹⁰, S. Malyukov³⁶, J. Mamuzic¹⁷⁴, G. Mancini⁵¹, I. Mandić⁹¹, L. Manhaes de Andrade Filho^{80a}, I.M. Maniatis¹⁶², J. Manjarres Ramos⁴⁸, K.H. Mankinen⁹⁶, A. Mann¹¹⁴, A. Manousos⁷⁶, B. Mansoulie¹⁴⁵, I. Manthos¹⁶², S. Manzoni¹²⁰, A. Marantis¹⁶², G. Marceca³⁰, L. Marchese¹³⁵, G. Marchiori¹³⁶, M. Marcisovsky¹⁴¹, C. Marcon⁹⁶, C.A. Marin Tobon³⁶, M. Marjanovic³⁸, F. Marroquim^{80b}, Z. Marshall¹⁸, M.U.F. Martensson¹⁷², S. Marti-Garcia¹⁷⁴, C.B. Martin¹²⁶, T.A. Martin¹⁷⁸, V.J. Martin⁵⁰, B. Martin dit Latour¹⁷, L. Martinelli^{74a,74b}, M. Martinez^{14,w}, V.I. Martinez Outschoorn¹⁰², S. Martin-Haugh¹⁴⁴, V.S. Martoiu^{27b}, A.C. Martyniuk⁹⁴, A. Marzin³⁶, L. Masetti⁹⁹, T. Mashimo¹⁶³, R. Mashinistov¹¹⁰, J. Masik¹⁰⁰, A.L. Maslennikov^{122b,122a}, L.H. Mason¹⁰⁴, L. Massa^{73a,73b}, P. Massarotti^{69a,69b}, P. Mastrandrea^{71a,71b}, A. Mastroberardino^{41b,41a}, T. Masubuchi¹⁶³, A. Matic¹¹⁴, P. Mättig²⁴, J. Maurer^{27b}, B. Maček⁹¹, S.J. Maxfield⁹⁰, D.A. Maximov^{122b,122a}, R. Mazini¹⁵⁸, I. Maznas¹⁶², S.M. Mazza¹⁴⁶, S.P. Mc Kee¹⁰⁵, T.G. McCarthy¹¹⁵, L.I. McClymont⁹⁴, W.P. McCormack¹⁸, E.F. McDonald¹⁰⁴, J.A. Mcfayden³⁶, M.A. McKay⁴², K.D. McLean¹⁷⁶, S.J. McMahon¹⁴⁴, P.C. McNamara¹⁰⁴, C.J. McNicol¹⁷⁸, R.A. McPherson^{176,ac}, J.E. Mdhluli^{33c}, Z.A. Meadows¹⁰², S. Meehan¹⁴⁸, T. Megy⁵², S. Mehlhase¹¹⁴, A. Mehta⁹⁰, T. Meideck⁵⁸, B. Meirose⁴³, D. Melini¹⁷⁴, B.R. Mellado Garcia^{33c}, J.D. Mellenthin⁵³, M. Melo^{28a}, F. Meloni⁴⁶, A. Melzer²⁴, S.B. Menary¹⁰⁰, E.D. Mendes Gouveia^{140a,140e}, L. Meng³⁶, X.T. Meng¹⁰⁵, S. Menke¹¹⁵, E. Meoni^{41b,41a}, S. Mergelmeyer¹⁹, S.A.M. Merkt¹³⁹, C. Merlassino²⁰, P. Mermod⁵⁴, L. Merola^{69a,69b}, C. Meroni^{68a}, O. Meshkov^{113,110}, J.K.R. Meshreki¹⁵¹, A. Messina^{72a,72b}, J. Metcalfe⁶, A.S. Mete¹⁷¹, C. Meyer⁶⁵, J. Meyer¹⁶⁰, J-P. Meyer¹⁴⁵, H. Meyer Zu Theenhausen^{61a}, F. Miano¹⁵⁶, R.P. Middleton¹⁴⁴, L. Mijović⁵⁰, G. Mikenberg¹⁸⁰, M. Mikestikova¹⁴¹, M. Mikuž⁹¹, H. Mildner¹⁴⁹, M. Milesi¹⁰⁴, A. Milic¹⁶⁷, D.A. Millar⁹², D.W. Miller³⁷, A. Milov¹⁸⁰, D.A. Milstead^{45a,45b}, R.A. Mina^{153,p}, A.A. Minaenko¹²³, M. Miñano Moya¹⁷⁴, I.A. Minashvili^{159b}, A.I. Mincer¹²⁴, B. Mindur^{83a}, M. Mineev⁷⁹, Y. Minegishi¹⁶³, Y. Ming¹⁸¹, L.M. Mir¹⁴, A. Mirto^{67a,67b}, K.P. Mistry¹³⁷, T. Mitani¹⁷⁹, J. Mitrevski¹¹⁴, V.A. Mitsou¹⁷⁴, M. Mittal^{60c}, A. Miucci²⁰, P.S. Miyagawa¹⁴⁹, A. Mizukami⁸¹, J.U. Mjörnmark⁹⁶, T. Mkrtchyan¹⁸⁴, M. Mlynarikova¹⁴³, T. Moa^{45a,45b}, K. Mochizuki¹⁰⁹, P. Mogg⁵², S. Mohapatra³⁹, R. Moles-Valls²⁴, M.C. Mondragon¹⁰⁶, K. Mönig⁴⁶, J. Monk⁴⁰, E. Monnier¹⁰¹, A. Montalbano¹⁵², J. Montejo Berlingen³⁶, M. Montella⁹⁴, F. Monticelli⁸⁸, S. Monzani^{68a}, N. Morange¹³², D. Moreno²², M. Moreno Llácer³⁶, P. Morettini^{55b}, M. Morgenstern¹²⁰, S. Morgenstern⁴⁸, D. Mori¹⁵², M. Morii⁵⁹, M. Morinaga¹⁷⁹, V. Morisbak¹³⁴, A.K. Morley³⁶, G. Mornacchi³⁶, A.P. Morris⁹⁴, L. Morvaj¹⁵⁵, P. Moschovakos¹⁰, B. Moser¹²⁰, M. Mosidze^{159b}, T. Moskalets¹⁴⁵, H.J. Moss¹⁴⁹, J. Moss^{31,m}, K. Motohashi¹⁶⁵, E. Mountricha³⁶, E.J.W. Moyse¹⁰², S. Muanza¹⁰¹, F. Mueller¹¹⁵, J. Mueller¹³⁹, R.S.P. Mueller¹¹⁴, D. Muenstermann⁸⁹, G.A. Mullier⁹⁶, J.L. Munoz Martinez¹⁴, F.J. Munoz Sanchez¹⁰⁰, P. Murin^{28b}, W.J. Murray^{178,144}, A. Murrone^{68a,68b}, M. Muškinja¹⁸, C. Mwewa^{33a}, A.G. Myagkov^{123,an}, J. Myers¹³¹, M. Myska¹⁴², B.P. Nachman¹⁸, O. Nackenhorst⁴⁷, A. Nag Nag⁴⁸, K. Nagai¹³⁵, K. Nagano⁸¹, Y. Nagasaka⁶², M. Nagel⁵², E. Nagy¹⁰¹, A.M. Nairz³⁶, Y. Nakahama¹¹⁷, K. Nakamura⁸¹, T. Nakamura¹⁶³, I. Nakano¹²⁷, H. Nanjo¹³³, F. Napolitano^{61a}, R.F. Naranjo Garcia⁴⁶, R. Narayan¹¹, D.I. Narrias Villar^{61a}, I. Naryshkin¹³⁸, T. Naumann⁴⁶, G. Navarro²², H.A. Neal^{105,*}, P.Y. Nechaeva¹¹⁰, F. Nechansky⁴⁶, T.J. Neep²¹, A. Negri^{70a,70b}, M. Negrini^{23b}, S. Nektarijevic¹¹⁹, C. Nellist⁵³, M.E. Nelson¹³⁵, S. Nemecek¹⁴¹, P. Nemethy¹²⁴, M. Nessi^{36,d}, M.S. Neubauer¹⁷³, M. Neumann¹⁸², P.R. Newman²¹, T.Y. Ng^{63c}, Y.S. Ng¹⁹, Y.W.Y. Ng¹⁷¹, H.D.N. Nguyen¹⁰¹, T. Nguyen Manh¹⁰⁹, E. Nibigira³⁸, R.B. Nickerson¹³⁵, R. Nicolaidou¹⁴⁵, D.S. Nielsen⁴⁰, J. Nielsen¹⁴⁶, N. Nikiforou¹¹, V. Nikolaenko^{123,an}, I. Nikolic-Audit¹³⁶, K. Nikolopoulos²¹, P. Nilsson²⁹, H.R. Nindhito⁵⁴, Y. Ninomiya⁸¹, A. Nisati^{72a}, N. Nishu^{60c}, R. Nisius¹¹⁵, I. Nitsche⁴⁷, T. Nitta¹⁷⁹, T. Nobe¹⁶³, Y. Noguchi⁸⁵, M. Nomachi¹³³, I. Nomidis¹³⁶, M.A. Nomura²⁹, M. Nordberg³⁶, N. Norjoharuddeen¹³⁵, T. Novak⁹¹, O. Novgorodova⁴⁸, R. Novotny¹⁴², L. Nozka¹³⁰, K. Ntekas¹⁷¹, E. Nurse⁹⁴, F. Nuti¹⁰⁴, F.G. Oakham^{34,aw}, H. Oberlack¹¹⁵, J. Ocariz¹³⁶, A. Ochi⁸², I. Ochoa³⁹, J.P. Ochoa-Ricoux^{147a}, K. O'Connor²⁶, S. Oda⁸⁷, S. Odaka⁸¹, S. Oerdek⁵³, A. Ogrodnik^{83a}, A. Oh¹⁰⁰, S.H. Oh⁴⁹, C.C. Ohm¹⁵⁴, H. Oide^{55b,55a}, M.L. Ojeda¹⁶⁷, H. Okawa¹⁶⁹, Y. Okazaki⁸⁵, Y. Okumura¹⁶³,

T. Okuyama⁸¹, A. Olariu^{27b}, L.F. Oleiro Seabra^{140a}, S.A. Olivares Pino^{147a}, D. Oliveira Damazio²⁹, J.L. Oliver¹, M.J.R. Olsson¹⁷¹, A. Olszewski⁸⁴, J. Olszowska⁸⁴, D.C. O'Neil¹⁵², A. Onofre^{140a,140e}, K. Onogi¹¹⁷, P.U.E. Onyisi¹¹, H. Oppen¹³⁴, M.J. Oreglia³⁷, G.E. Orellana⁸⁸, Y. Oren¹⁶¹, D. Orestano^{74a,74b}, N. Orlando¹⁴, R.S. Orr¹⁶⁷, V. O'Shea⁵⁷, R. Ospanov^{60a}, G. Otero y Garzon³⁰, H. Otono⁸⁷, M. Ouchrif^{35d}, F. Ould-Saada¹³⁴, A. Ouraou¹⁴⁵, Q. Ouyang^{15a}, M. Owen⁵⁷, R.E. Owen²¹, V.E. Ozcan^{12c}, N. Ozturk⁸, J. Pacalt¹³⁰, H.A. Pacey³², K. Pachal⁴⁹, A. Pacheco Pages¹⁴, C. Padilla Aranda¹⁴, S. Pagan Griso¹⁸, M. Paganini¹⁸³, G. Palacino⁶⁵, S. Palazzo⁵⁰, S. Palestini³⁶, M. Palka^{83b}, D. Pallin³⁸, I. Panagoulas¹⁰, C.E. Pandini³⁶, J.G. Panduro Vazquez⁹³, P. Pani⁴⁶, G. Panizzo^{66a,66c}, L. Paolozzi⁵⁴, C. Papadatos¹⁰⁹, K. Papageorgiou^{9,h}, A. Paramonov⁶, D. Paredes Hernandez^{63b}, S.R. Paredes Saenz¹³⁵, B. Parida¹⁶⁶, T.H. Park¹⁶⁷, A.J. Parker⁸⁹, M.A. Parker³², F. Parodi^{55b,55a}, E.W.P. Parrish¹²¹, J.A. Parsons³⁹, U. Parzefall⁵², L. Pascual Dominguez¹³⁶, V.R. Pascuzzi¹⁶⁷, J.M.P. Pasner¹⁴⁶, E. Pasqualucci^{72a}, S. Passaggio^{55b}, F. Pastore⁹³, P. Pasuwan^{45a,45b}, S. Patariaia⁹⁹, J.R. Pater¹⁰⁰, A. Pathak¹⁸¹, T. Pauly³⁶, B. Pearson¹¹⁵, M. Pedersen¹³⁴, L. Pedraza Diaz¹¹⁹, R. Pedro^{140a,140b}, T. Peiffer⁵³, S.V. Peleganchuk^{122b,122a}, O. Penc¹⁴¹, H. Peng^{60a}, B.S. Peralva^{80a}, M.M. Perego¹³², A.P. Pereira Peixoto^{140a,140e}, D.V. Perepelitsa²⁹, F. Peri¹⁹, L. Perini^{68a,68b}, H. Pernegger³⁶, S. Perrella^{69a,69b}, V.D. Peshekhonov^{79,*}, K. Peters⁴⁶, R.F.Y. Peters¹⁰⁰, B.A. Petersen³⁶, T.C. Petersen⁴⁰, E. Petit⁵⁸, A. Petridis¹, C. Petridou¹⁶², P. Petroff¹³², M. Petrov¹³⁵, F. Petrucci^{74a,74b}, M. Pettee¹⁸³, N.E. Pettersson¹⁰², K. Petukhova¹⁴³, A. Peyaud¹⁴⁵, R. Pezoa^{147b}, L. Pezzotti^{70a,70b}, T. Pham¹⁰⁴, F.H. Phillips¹⁰⁶, P.W. Phillips¹⁴⁴, M.W. Phipps¹⁷³, G. Piacquadio¹⁵⁵, E. Pianori¹⁸, A. Picazio¹⁰², R.H. Pickles¹⁰⁰, R. Piegai³⁰, D. Pietreanu^{27b}, J.E. Pilcher³⁷, A.D. Pilkington¹⁰⁰, M. Pinamonti^{73a,73b}, J.L. Pinfold³, M. Pitt¹⁸⁰, L. Pizzimento^{73a,73b}, M.-A. Pleier²⁹, V. Pleskot¹⁴³, E. Plotnikova⁷⁹, D. Pluth⁷⁸, P. Podberezko^{122b,122a}, R. Poettgen⁹⁶, R. Poggi⁵⁴, L. Poggioli¹³², I. Pogrebnyak¹⁰⁶, D. Pohl²⁴, I. Pokharel⁵³, G. Polesello^{70a}, A. Poley¹⁸, A. Policicchio^{72a,72b}, R. Polifka³⁶, A. Polini^{23b}, C.S. Pollard⁴⁶, V. Polychronakos²⁹, D. Ponomarenko¹¹², L. Pontecorvo³⁶, S. Popa^{27a}, G.A. Popeneciu^{27d}, D.M. Portillo Quintero⁵⁸, S. Pospisil¹⁴², K. Potamianos⁴⁶, I.N. Potrap⁷⁹, C.J. Potter³², H. Potti¹¹, T. Poulsen⁹⁶, J. Poveda³⁶, T.D. Powell¹⁴⁹, G. Pownall⁴⁶, M.E. Pozo Astigarraga³⁶, P. Pralavorio¹⁰¹, S. Prell⁷⁸, D. Price¹⁰⁰, M. Primavera^{67a}, S. Prince¹⁰³, M.L. Proffitt¹⁴⁸, N. Proklova¹¹², K. Prokofiev^{63c}, F. Prokoshin^{147b}, S. Protopopescu²⁹, J. Proudfoot⁶, M. Przybycien^{83a}, A. Puri¹⁷³, P. Puzo¹³², J. Qian¹⁰⁵, Y. Qin¹⁰⁰, A. Quadt⁵³, M. Queitsch-Maitland⁴⁶, A. Qureshi¹, P. Rados¹⁰⁴, F. Ragusa^{68a,68b}, G. Rahal⁹⁷, J.A. Raine⁵⁴, S. Rajagopalan²⁹, A. Ramirez Morales⁹², K. Ran^{15a,15d}, T. Rashid¹³², S. Raspopov⁵, M.G. Ratti^{68a,68b}, D.M. Rauch⁴⁶, F. Rauscher¹¹⁴, S. Rave⁹⁹, B. Ravina¹⁴⁹, I. Ravinovich¹⁸⁰, J.H. Rawling¹⁰⁰, M. Raymond³⁶, A.L. Read¹³⁴, N.P. Readioff⁵⁸, M. Reale^{67a,67b}, D.M. Rebuzzi^{70a,70b}, A. Redelbach¹⁷⁷, G. Redlinger²⁹, R.G. Reed^{33c}, K. Reeves⁴³, L. Rehnisch¹⁹, J. Reichert¹³⁷, D. Reikher¹⁶¹, A. Reiss⁹⁹, A. Rej¹⁵¹, C. Rembser³⁶, M. Renda^{27b}, M. Rescigno^{72a}, S. Resconi^{68a}, E.D. Resseguie¹³⁷, S. Rettie¹⁷⁵, E. Reynolds²¹, O.L. Rezanova^{122b,122a}, P. Reznicek¹⁴³, E. Ricci^{75a,75b}, R. Richter¹¹⁵, S. Richter⁴⁶, E. Richter-Was^{83b}, O. Ricken²⁴, M. Ridel¹³⁶, P. Rieck¹¹⁵, C.J. Riegel¹⁸², O. Rifki⁴⁶, M. Rijssenbeek¹⁵⁵, A. Rimoldi^{70a,70b}, M. Rimoldi²⁰, L. Rinaldi^{23b}, G. Ripellino¹⁵⁴, B. Ristić⁸⁹, E. Ritsch³⁶, I. Riu¹⁴, J.C. Rivera Vergara^{147a}, F. Rizatdinova¹²⁹, E. Rizvi⁹², C. Rizzi³⁶, R.T. Roberts¹⁰⁰, S.H. Robertson^{103,ac}, M. Robin⁴⁶, D. Robinson³², J.E.M. Robinson⁴⁶, A. Robson⁵⁷, E. Rocco⁹⁹, C. Roda^{71a,71b}, Y. Rodina¹⁰¹, S. Rodriguez Bosca¹⁷⁴, A. Rodriguez Perez¹⁴, D. Rodriguez Rodriguez¹⁷⁴, A.M. Rodríguez Vera^{168b}, S. Roe³⁶, O. Röhne¹³⁴, R. Röhrig¹¹⁵, C.P.A. Roland⁶⁵, J. Roloff⁵⁹, A. Romaniouk¹¹², M. Romano^{23b,23a}, N. Rompotis⁹⁰, M. Ronzani¹²⁴, L. Roos¹³⁶, S. Rosati^{72a}, K. Rosbach⁵², N.-A. Rosien⁵³, G. Rosin¹⁰², B.J. Rosser¹³⁷, E. Rossi⁴⁶, E. Rossi^{74a,74b}, E. Rossi^{69a,69b}, L.P. Rossi^{55b}, L. Rossini^{68a,68b}, J.H.N. Rosten³², R. Rosten¹⁴, M. Rotaru^{27b}, J. Rothberg¹⁴⁸, D. Rousseau¹³², G. Rovelli^{70a,70b}, D. Roy^{33c}, A. Rozanov¹⁰¹, Y. Rozen¹⁶⁰, X. Ruan^{33c}, F. Rubbo¹⁵³, F. Rühr⁵², A. Ruiz-Martinez¹⁷⁴, A. Rummler³⁶, Z. Rurikova⁵², N.A. Rusakovich⁷⁹, H.L. Russell¹⁰³, L. Rustige^{38,47}, J.P. Rutherford⁷, E.M. Rüttinger^{46,j}, Y.F. Ryabov¹³⁸, M. Rybar³⁹, G. Rybkin¹³², A. Ryzhov¹²³, G.F. Rzehorz⁵³, P. Sabatini⁵³, G. Sabato¹²⁰, S. Sacerdoti¹³², H.F.-W. Sadrozinski¹⁴⁶, R. Sadykov⁷⁹, F. Safai Tehrani^{72a}, B. Safarzadeh Samani¹⁵⁶, P. Saha¹²¹, S. Saha¹⁰³, M. Sahinsoy^{61a}, A. Sahu¹⁸², M. Saimpert⁴⁶, M. Saito¹⁶³, T. Saito¹⁶³, H. Sakamoto¹⁶³, A. Sakharov^{124,am}, D. Salamani⁵⁴, G. Salamanna^{74a,74b}, J.E. Salazar Loyola^{147b}, P.H. Sales De Bruin¹⁷², D. Salihagic^{115,*}, A. Salnikov¹⁵³, J. Salt¹⁷⁴, D. Salvatore^{41b,41a}, F. Salvatore¹⁵⁶, A. Salvucci^{63a,63b,63c}, A. Salzburger³⁶, J. Samarati³⁶,

D. Sammel⁵², D. Sampsonidis¹⁶², D. Sampsonidou¹⁶², J. Sánchez¹⁷⁴, A. Sanchez Pineda^{66a,66c},
H. Sandaker¹³⁴, C.O. Sander⁴⁶, I.G. Sanderswood⁸⁹, M. Sandhoff¹⁸², C. Sandoval²², D.P.C. Sankey¹⁴⁴,
M. Sannino^{55b,55a}, Y. Sano¹¹⁷, A. Sansoni⁵¹, C. Santoni³⁸, H. Santos^{140a,140b}, S.N. Santpur¹⁸,
A. Santra¹⁷⁴, A. Saproinov⁷⁹, J.G. Saraiva^{140a,140d}, O. Sasaki⁸¹, K. Sato¹⁶⁹, E. Sauvan⁵, P. Savard^{167,aw},
N. Savic¹¹⁵, R. Sawada¹⁶³, C. Sawyer¹⁴⁴, L. Sawyer^{95,ak}, C. Sbarra^{23b}, A. Sbrizzi^{23a}, T. Scanlon⁹⁴,
J. Schaarschmidt¹⁴⁸, P. Schacht¹¹⁵, B.M. Schachtner¹¹⁴, D. Schaefer³⁷, L. Schaefer¹³⁷, J. Schaeffer⁹⁹,
S. Schaepe³⁶, U. Schäfer⁹⁹, A.C. Schaffer¹³², D. Schaile¹¹⁴, R.D. Schamberger¹⁵⁵, N. Scharmberg¹⁰⁰,
V.A. Schegelsky¹³⁸, D. Scheirich¹⁴³, F. Schenck¹⁹, M. Schernau¹⁷¹, C. Schiavi^{55b,55a}, S. Schier¹⁴⁶,
L.K. Schildgen²⁴, Z.M. Schillaci²⁶, E.J. Schioppa³⁶, M. Schioppa^{41b,41a}, K.E. Schleicher⁵², S. Schlenker³⁶,
K.R. Schmidt-Sommerfeld¹¹⁵, K. Schmieden³⁶, C. Schmitt⁹⁹, S. Schmitt⁴⁶, S. Schmitz⁹⁹,
J.C. Schmoeckel⁴⁶, U. Schnoor⁵², L. Schoeffel¹⁴⁵, A. Schoening^{61b}, E. Schopf¹³⁵, M. Schott⁹⁹,
J.F.P. Schouwenberg¹¹⁹, J. Schovancova³⁶, S. Schramm⁵⁴, F. Schroeder¹⁸², A. Schulte⁹⁹,
H.-C. Schultz-Coulon^{61a}, M. Schumacher⁵², B.A. Schumm¹⁴⁶, Ph. Schune¹⁴⁵, A. Schwartzman¹⁵³,
T.A. Schwarz¹⁰⁵, Ph. Schwemling¹⁴⁵, R. Schwiendhorst¹⁰⁶, A. Sciandra¹⁴⁶, G. Sciolla²⁶, M. Scodeggio⁴⁶,
M. Scornajenghi^{41b,41a}, F. Scuri^{71a}, F. Scutti¹⁰⁴, L.M. Scyboz¹¹⁵, C.D. Sebastiani^{72a,72b}, P. Seema¹⁹,
S.C. Seidel¹¹⁸, A. Seiden¹⁴⁶, T. Seiss³⁷, J.M. Seixas^{80b}, G. Sekhniaidze^{69a}, K. Sekhon¹⁰⁵, S.J. Sekula⁴²,
N. Semprini-Cesari^{23b,23a}, S. Sen⁴⁹, S. Senkin³⁸, C. Serfon⁷⁶, L. Serin¹³², L. Serkin^{66a,66b}, M. Sessa^{60a},
H. Severini¹²⁸, F. Sforza¹⁷⁰, A. Sfyrla⁵⁴, E. Shabalina⁵³, J.D. Shahinian¹⁴⁶, N.W. Shaikh^{45a,45b},
D. Shaked Renous¹⁸⁰, L.Y. Shan^{15a}, R. Shang¹⁷³, J.T. Shank²⁵, M. Shapiro¹⁸, A. Sharma¹³⁵, A.S. Sharma¹,
P.B. Shatalov¹¹¹, K. Shaw¹⁵⁶, S.M. Shaw¹⁰⁰, A. Shcherbakova¹³⁸, Y. Shen¹²⁸, N. Sherafati³⁴,
A.D. Sherman²⁵, P. Sherwood⁹⁴, L. Shi^{158,as}, S. Shimizu⁸¹, C.O. Shimmin¹⁸³, Y. Shimogama¹⁷⁹,
M. Shimojima¹¹⁶, I.P.J. Shipsey¹³⁵, S. Shirabe⁸⁷, M. Shiyakova^{79,z}, J. Shlomi¹⁸⁰, A. Shmeleva¹¹⁰,
M.J. Shochet³⁷, S. Shojaii¹⁰⁴, D.R. Shope¹²⁸, S. Shrestha¹²⁶, E. Shulga¹⁸⁰, P. Sicho¹⁴¹, A.M. Sickles¹⁷³,
P.E. Sidebo¹⁵⁴, E. Sideras Haddad^{33c}, O. Sidiropoulou³⁶, A. Sidoti^{23b,23a}, F. Siegert⁴⁸, Dj. Sijacki¹⁶,
M. Silva Jr.¹⁸¹, M.V. Silva Oliveira^{80a}, S.B. Silverstein^{45a}, S. Simion¹³², E. Simioni⁹⁹, M. Simon⁹⁹,
R. Simoniello⁹⁹, P. Sinervo¹⁶⁷, N.B. Sinev¹³¹, M. Sioli^{23b,23a}, I. Siral¹⁰⁵, S.Yu. Sivoklov¹¹³,
J. Sjölin^{45a,45b}, E. Skorda⁹⁶, P. Skubic¹²⁸, M. Slawinska⁸⁴, K. Sliwa¹⁷⁰, R. Slovak¹⁴³, V. Smakhtin¹⁸⁰,
B.H. Smart¹⁴⁴, J. Smiesko^{28a}, N. Smirnov¹¹², S.Yu. Smirnov¹¹², Y. Smirnov¹¹², L.N. Smirnova^{113,s},
O. Smirnova⁹⁶, J.W. Smith⁵³, M. Smizanska⁸⁹, K. Smolek¹⁴², A. Smykiewicz⁸⁴, A.A. Snesarev¹¹⁰,
H.L. Snoek¹²⁰, I.M. Snyder¹³¹, S. Snyder²⁹, R. Sobie^{176,ac}, A.M. Soffa¹⁷¹, A. Soffer¹⁶¹, A. Sogaard⁵⁰,
F. Sohns⁵³, G. Sokhrannyi⁹¹, C.A. Solans Sanchez³⁶, E.Yu. Soldatov¹¹², U. Soldevila¹⁷⁴, A.A. Solodkov¹²³,
A. Soloshenko⁷⁹, O.V. Solovyanov¹²³, V. Solovyev¹³⁸, P. Sommer¹⁴⁹, H. Son¹⁷⁰, W. Song¹⁴⁴,
W.Y. Song^{168b}, A. Sopczak¹⁴², F. Sopkova^{28b}, C.L. Sotiropoulou^{71a,71b}, S. Sottocornola^{70a,70b},
R. Soualah^{66a,66c,g}, A.M. Soukharev^{122b,122a}, D. South⁴⁶, S. Spagnolo^{67a,67b}, M. Spalla¹¹⁵,
M. Spangenberg¹⁷⁸, F. Spanò⁹³, D. Sperlich⁵², T.M. Spieker^{61a}, R. Spighi^{23b}, G. Spigo³⁶, L.A. Spiller¹⁰⁴,
M. Spina¹⁵⁶, D.P. Spiteri⁵⁷, M. Spousta¹⁴³, A. Stabile^{68a,68b}, B.L. Stamas¹²¹, R. Stamen^{61a},
M. Stamenkovic¹²⁰, S. Stamm¹⁹, E. Stanecka⁸⁴, R.W. Stanek⁶, B. Stanislaus¹³⁵, M.M. Stanitzki⁴⁶,
M. Stankaityte¹³⁵, B. Stapf¹²⁰, E.A. Starchenko¹²³, G.H. Stark¹⁴⁶, J. Stark⁵⁸, S.H. Stark⁴⁰, P. Staroba¹⁴¹,
P. Starovoitov^{61a}, S. Stärz¹⁰³, R. Staszewski⁸⁴, G. Stavropoulos⁴⁴, M. Stegler⁴⁶, P. Steinberg²⁹,
A.L. Steinhebel¹³¹, B. Stelzer¹⁵², H.J. Stelzer³⁶, O. Stelzer-Chilton^{168a}, H. Stenzel⁵⁶, T.J. Stevenson¹⁵⁶,
G.A. Stewart³⁶, M.C. Stockton³⁶, G. Stoica^{27b}, M. Stolarski^{140a}, P. Stolte⁵³, S. Stonjek¹¹⁵,
A. Straessner⁴⁸, J. Strandberg¹⁵⁴, S. Strandberg^{45a,45b}, M. Strauss¹²⁸, P. Strizenec^{28b}, R. Ströhmer¹⁷⁷,
D.M. Strom¹³¹, R. Stroynowski⁴², A. Strubig⁵⁰, S.A. Stucci²⁹, B. Stugu¹⁷, J. Stupak¹²⁸, N.A. Styles⁴⁶,
D. Su¹⁵³, S. Suchek^{61a}, Y. Sugaya¹³³, V.V. Sulin¹¹⁰, M.J. Sullivan⁹⁰, D.M.S. Sultan⁵⁴, S. Sultansoy^{4c},
T. Sumida⁸⁵, S. Sun¹⁰⁵, X. Sun³, K. Suruliz¹⁵⁶, C.J.E. Suster¹⁵⁷, M.R. Sutton¹⁵⁶, S. Suzuki⁸¹, M. Svatos¹⁴¹,
M. Swiatlowski³⁷, S.P. Swift², A. Sydorenko⁹⁹, I. Sykora^{28a}, M. Sykora¹⁴³, T. Sykora¹⁴³, D. Ta⁹⁹,
K. Tackmann^{46,x}, J. Taenzer¹⁶¹, A. Taffard¹⁷¹, R. Tafirout^{168a}, E. Tahirovic⁹², H. Takai²⁹, R. Takashima⁸⁶,
K. Takeda⁸², T. Takeshita¹⁵⁰, E.P. Takeva⁵⁰, Y. Takubo⁸¹, M. Talby¹⁰¹, A.A. Talyshev^{122b,122a},
N.M. Tamir¹⁶¹, J. Tanaka¹⁶³, M. Tanaka¹⁶⁵, R. Tanaka¹³², B.B. Tannenwald¹²⁶, S. Tapia Araya¹⁷³,
S. Tapprogge⁹⁹, A. Tarek Abouelfadl Mohamed¹³⁶, S. Tarem¹⁶⁰, G. Tarna^{27b,c}, G.F. Tartarelli^{68a}, P. Tas¹⁴³,
M. Tasevsky¹⁴¹, T. Tashiro⁸⁵, E. Tassi^{41b,41a}, A. Tavares Delgado^{140a,140b}, Y. Tayalati^{35e}, A.J. Taylor⁵⁰,
G.N. Taylor¹⁰⁴, P.T.E. Taylor¹⁰⁴, W. Taylor^{168b}, A.S. Tee⁸⁹, R. Teixeira De Lima¹⁵³, P. Teixeira-Dias⁹³,

H. Ten Kate³⁶, J.J. Teoh¹²⁰, S. Terada⁸¹, K. Terashi¹⁶³, J. Terron⁹⁸, S. Terzo¹⁴, M. Testa⁵¹,
R.J. Teuscher^{167,ac}, S.J. Thais¹⁸³, T. Theveneaux-Pelzer⁴⁶, F. Thiele⁴⁰, D.W. Thomas⁹³, J.O. Thomas⁴²,
J.P. Thomas²¹, A.S. Thompson⁵⁷, P.D. Thompson²¹, L.A. Thomsen¹⁸³, E. Thomson¹³⁷, Y. Tian³⁹,
R.E. Ticse Torres⁵³, V.O. Tikhomirov^{110,ao}, Yu.A. Tikhonov^{122b,122a}, S. Timoshenko¹¹², P. Tipton¹⁸³,
S. Tisserant¹⁰¹, K. Todome^{23b,23a}, S. Todorova-Nova⁵, S. Todt⁴⁸, J. Tojo⁸⁷, S. Tokár^{28a}, K. Tokushuku⁸¹,
E. Tolley¹²⁶, K.G. Tomiwa^{33c}, M. Tomoto¹¹⁷, L. Tompkins^{153,p}, K. Toms¹¹⁸, B. Tong⁵⁹, P. Tornambe¹⁰²,
E. Torrence¹³¹, H. Torres⁴⁸, E. Torró Pastor¹⁴⁸, C. Toscirci¹³⁵, J. Toth^{101,aa}, D.R. Tovey¹⁴⁹, C.J. Treado¹²⁴,
T. Trefzger¹⁷⁷, F. Tresoldi¹⁵⁶, A. Tricoli²⁹, I.M. Trigger^{168a}, S. Trincaz-Duvold¹³⁶, W. Trischuk¹⁶⁷,
B. Trocme⁵⁸, A. Trofymov¹³², C. Troncon^{68a}, M. Trovatelli¹⁷⁶, F. Trovato¹⁵⁶, L. Truong^{33b},
M. Trzebinski⁸⁴, A. Trzupek⁸⁴, F. Tsai⁴⁶, J.C.-L. Tseng¹³⁵, P.V. Tsiareshka^{107,ai}, A. Tsigotis¹⁶²,
N. Tsirintanis⁹, V. Tsiskaridze¹⁵⁵, E.G. Tskhadadze^{159a}, M. Tsopoulou¹⁶², I.I. Tsukerman¹¹¹, V. Tsulaia¹⁸,
S. Tsuno⁸¹, D. Tsybychev¹⁵⁵, Y. Tu^{63b}, A. Tudorache^{27b}, V. Tudorache^{27b}, T.T. Tulbure^{27a}, A.N. Tuna⁵⁹,
S. Turchikhin⁷⁹, D. Turgeman¹⁸⁰, I. Turk Cakir^{4b,t}, R.J. Turner²¹, R.T. Turra^{68a}, P.M. Tuts³⁹,
S. Tzamarias¹⁶², E. Tzovara⁹⁹, G. Uccielli⁴⁷, I. Ueda⁸¹, M. Ughetto^{45a,45b}, F. Ukegawa¹⁶⁹, G. Unal³⁶,
A. Undrus²⁹, G. Unel¹⁷¹, F.C. Ungaro¹⁰⁴, Y. Unno⁸¹, K. Uno¹⁶³, J. Urban^{28b}, P. Urquijo¹⁰⁴, G. Usai⁸,
J. Usui⁸¹, L. Vacavant¹⁰¹, V. Vacek¹⁴², B. Vachon¹⁰³, K.O.H. Vadla¹³⁴, A. Vaidya⁹⁴, C. Valderanis¹¹⁴,
E. Valdes Santurio^{45a,45b}, M. Valente⁵⁴, S. Valentinetti^{23b,23a}, A. Valero¹⁷⁴, L. Valéry⁴⁶, R.A. Vallance²¹,
A. Vallier³⁶, J.A. Valls Ferrer¹⁷⁴, T.R. Van Daalen¹⁴, P. Van Gemmeren⁶, I. Van Vulpen¹²⁰,
M. Vanadia^{73a,73b}, W. Vandelli³⁶, A. Vaniachine¹⁶⁶, D. Vannicola^{72a,72b}, R. Vari^{72a}, E.W. Varnes⁷,
C. Varni^{55b,55a}, T. Varol⁴², D. Varouchas¹³², K.E. Varvell¹⁵⁷, M.E. Vasile^{27b}, G.A. Vasquez¹⁷⁶,
J.G. Vasquez¹⁸³, F. Vazeille³⁸, D. Vazquez Furelos¹⁴, T. Vazquez Schroeder³⁶, J. Veatch⁵³,
V. Vecchio^{74a,74b}, M.J. Veen¹²⁰, L.M. Veloce¹⁶⁷, F. Veloso^{140a,140c}, S. Veneziano^{72a}, A. Ventura^{67a,67b},
N. Venturi³⁶, A. Verbitskyi¹¹⁵, V. Vercesi^{70a}, M. Verducci^{74a,74b}, C.M. Vergel Infante⁷⁸, C. Vergis²⁴,
W. Verkerke¹²⁰, A.T. Vermeulen¹²⁰, J.C. Vermeulen¹²⁰, M.C. Vetterli^{152,aw}, N. Viaux Maira^{147b},
M. Vicente Barreto Pinto⁵⁴, I. Vichou^{173,*}, T. Vickey¹⁴⁹, O.E. Vickey Boeriu¹⁴⁹, G.H.A. Viehhauser¹³⁵,
L. Vignani¹³⁵, M. Villa^{23b,23a}, M. Villaplana Perez^{68a,68b}, E. Vilucchi⁵¹, M.G. Vincet³⁴, V.B. Vinogradov⁷⁹,
A. Vishwakarma⁴⁶, C. Vittori^{23b,23a}, I. Vivarelli¹⁵⁶, M. Vogel¹⁸², P. Vokac¹⁴², G. Volpi¹⁴,
S.E. von Buddenbrock^{33c}, E. Von Toerne²⁴, V. Vorobel¹⁴³, K. Vorobev¹¹², M. Vos¹⁷⁴, J.H. Vosseveld⁹⁰,
N. Vranjes¹⁶, M. Vranjes Milosavljevic¹⁶, V. Vrba¹⁴², M. Vreeswijk¹²⁰, T. Šfiligoj⁹¹, R. Vuillermet³⁶,
I. Vukotic³⁷, T. Ženiš^{28a}, L. Živković¹⁶, P. Wagner²⁴, W. Wagner¹⁸², J. Wagner-Kuhr¹¹⁴, H. Wahlberg⁸⁸,
K. Wakamiya⁸², V.M. Walbrecht¹¹⁵, J. Walder⁸⁹, R. Walker¹¹⁴, S.D. Walker⁹³, W. Walkowiak¹⁵¹,
V. Wallangen^{45a,45b}, A.M. Wang⁵⁹, C. Wang^{60b}, F. Wang¹⁸¹, H. Wang¹⁸, H. Wang³, J. Wang¹⁵⁷,
J. Wang^{61b}, P. Wang⁴², Q. Wang¹²⁸, R.-J. Wang⁹⁹, R. Wang^{60a}, R. Wang⁶, S.M. Wang¹⁵⁸, W.T. Wang^{60a},
W. Wang^{15c,ad}, W.X. Wang^{60a,ad}, Y. Wang^{60a,al}, Z. Wang^{60c}, C. Wanotayaroj⁴⁶, A. Warburton¹⁰³,
C.P. Ward³², D.R. Wardrope⁹⁴, A. Washbrook⁵⁰, A.T. Watson²¹, M.F. Watson²¹, G. Watts¹⁴⁸,
B.M. Waugh⁹⁴, A.F. Webb¹¹, S. Webb⁹⁹, C. Weber¹⁸³, M.S. Weber²⁰, S.A. Weber³⁴, S.M. Weber^{61a},
A.R. Weidberg¹³⁵, J. Weingarten⁴⁷, M. Weirich⁹⁹, C. Weiser⁵², P.S. Wells³⁶, T. Wenaus²⁹, T. Wengler³⁶,
S. Wenig³⁶, N. Wermes²⁴, M.D. Werner⁷⁸, P. Werner³⁶, M. Wessels^{61a}, T.D. Weston²⁰, K. Whalen¹³¹,
N.L. Whallon¹⁴⁸, A.M. Wharton⁸⁹, A.S. White¹⁰⁵, A. White⁸, M.J. White¹, R. White^{147b}, D. Whiteson¹⁷¹,
B.W. Whitmore⁸⁹, F.J. Wickens¹⁴⁴, W. Wiedenmann¹⁸¹, M. Wielers¹⁴⁴, N. Wieseotte⁹⁹,
C. Wigglesworth⁴⁰, L.A.M. Wiik-Fuchs⁵², F. Wilk¹⁰⁰, H.G. Wilkens³⁶, L.J. Wilkins⁹³, H.H. Williams¹³⁷,
S. Williams³², C. Willis¹⁰⁶, S. Willocq¹⁰², J.A. Wilson²¹, I. Wingerter-Seetz⁵, E. Winkels¹⁵⁶,
F. Winklmeier¹³¹, O.J. Winston¹⁵⁶, B.T. Winter⁵², M. Wittgen¹⁵³, M. Wobisch⁹⁵, A. Wolf⁹⁹,
T.M.H. Wolf¹²⁰, R. Wolff¹⁰¹, R.W. Wölke¹³⁵, J. Wollrath⁵², M.W. Wolter⁸⁴, H. Wolters^{140a,140c},
V.W.S. Wong¹⁷⁵, N.L. Woods¹⁴⁶, S.D. Worm²¹, B.K. Wosiek⁸⁴, K.W. Woźniak⁸⁴, K. Wraight⁵⁷,
S.L. Wu¹⁸¹, X. Wu⁵⁴, Y. Wu^{60a}, T.R. Wyatt¹⁰⁰, B.M. Wynne⁵⁰, S. Xella⁴⁰, Z. Xi¹⁰⁵, L. Xia¹⁷⁸, D. Xu^{15a},
H. Xu^{60a,c}, L. Xu²⁹, T. Xu¹⁴⁵, W. Xu¹⁰⁵, Z. Xu^{60b}, Z. Xu¹⁵³, B. Yabsley¹⁵⁷, S. Yacoub^{33a}, K. Yajima¹³³,
D.P. Yallup⁹⁴, D. Yamaguchi¹⁶⁵, Y. Yamaguchi¹⁶⁵, A. Yamamoto⁸¹, T. Yamanaka¹⁶³, F. Yamane⁸²,
M. Yamatani¹⁶³, T. Yamazaki¹⁶³, Y. Yamazaki⁸², Z. Yan²⁵, H.J. Yang^{60c,60d}, H.T. Yang¹⁸, S. Yang⁷⁷,
X. Yang^{60b,58}, Y. Yang¹⁶³, Z. Yang¹⁷, W.-M. Yao¹⁸, Y.C. Yap⁴⁶, Y. Yasu⁸¹, E. Yatsenko^{60c,60d}, J. Ye⁴²,
S. Ye²⁹, I. Yeletsikh⁷⁹, M.R. Yexley⁸⁹, E. Yigitbasi²⁵, E. Yildirim⁹⁹, K. Yorita¹⁷⁹, K. Yoshihara¹³⁷,
C.J.S. Young³⁶, C. Young¹⁵³, J. Yu⁷⁸, R. Yuan^{60b}, X. Yue^{61a}, S.P.Y. Yuen²⁴, B. Zabinski⁸⁴, G. Zacharis¹⁰,

E. Zaffaroni⁵⁴, J. Zahreddine¹³⁶, R. Zaidan¹⁴, A.M. Zaitsev^{123,an}, T. Zakareishvili^{159b}, N. Zakharchuk³⁴, S. Zambito⁵⁹, D. Zanzi³⁶, D.R. Zaripovas⁵⁷, S.V. Zeiðner⁴⁷, C. Zeitnitz¹⁸², G. Zemaityte¹³⁵, J.C. Zeng¹⁷³, O. Zenin¹²³, D. Zerwas¹³², M. Zgubič¹³⁵, D.F. Zhang^{15b}, F. Zhang¹⁸¹, G. Zhang^{60a}, G. Zhang^{15b}, H. Zhang^{15c}, J. Zhang⁶, L. Zhang^{15c}, L. Zhang^{60a}, M. Zhang¹⁷³, R. Zhang^{60a}, R. Zhang²⁴, X. Zhang^{60b}, Y. Zhang^{15a,15d}, Z. Zhang^{63a}, Z. Zhang¹³², P. Zhao⁴⁹, Y. Zhao^{60b}, Z. Zhao^{60a}, A. Zhemchugov⁷⁹, Z. Zheng¹⁰⁵, D. Zhong¹⁷³, B. Zhou¹⁰⁵, C. Zhou¹⁸¹, M.S. Zhou^{15a,15d}, M. Zhou¹⁵⁵, N. Zhou^{60c}, Y. Zhou⁷, C.G. Zhu^{60b}, H.L. Zhu^{60a}, H. Zhu^{15a}, J. Zhu¹⁰⁵, Y. Zhu^{60a}, X. Zhuang^{15a}, K. Zhukov¹¹⁰, V. Zhulanov^{122b,122a}, D. Zieminska⁶⁵, N.I. Zimine⁷⁹, S. Zimmermann⁵², Z. Zinonos¹¹⁵, M. Ziolkowski¹⁵¹, G. Zobernig¹⁸¹, A. Zoccoli^{23b,23a}, K. Zoch⁵³, T.G. Zorbas¹⁴⁹, R. Zou³⁷, L. Zwalinski³⁶

¹ Department of Physics, University of Adelaide, Adelaide, Australia

² Physics Department, SUNY Albany, Albany, NY, United States of America

³ Department of Physics, University of Alberta, Edmonton, AB, Canada

⁴ (a) Department of Physics, Ankara University, Ankara; (b) Istanbul Aydin University, Istanbul; (c) Division of Physics, TOBB University of Economics and Technology, Ankara, Turkey

⁵ LAPP, Université Grenoble Alpes, Université Savoie Mont Blanc, CNRS/IN2P3, Annecy, France

⁶ High Energy Physics Division, Argonne National Laboratory, Argonne, IL, United States of America

⁷ Department of Physics, University of Arizona, Tucson, AZ, United States of America

⁸ Department of Physics, University of Texas at Arlington, Arlington, TX, United States of America

⁹ Physics Department, National and Kapodistrian University of Athens, Athens, Greece

¹⁰ Physics Department, National Technical University of Athens, Zografou, Greece

¹¹ Department of Physics, University of Texas at Austin, Austin, TX, United States of America

¹² (a) Bahcesehir University, Faculty of Engineering and Natural Sciences, Istanbul; (b) Istanbul Bilgi University, Faculty of Engineering and Natural Sciences, Istanbul; (c) Department of Physics, Bogazici University, Istanbul; (d) Department of Physics Engineering, Gaziantep University, Gaziantep, Turkey

¹³ Institute of Physics, Azerbaijan Academy of Sciences, Baku, Azerbaijan

¹⁴ Institut de Física d'Altes Energies (IFAE), Barcelona Institute of Science and Technology, Barcelona, Spain

¹⁵ (a) Institute of High Energy Physics, Chinese Academy of Sciences, Beijing; (b) Physics Department, Tsinghua University, Beijing; (c) Department of Physics, Nanjing University, Nanjing;

(d) University of Chinese Academy of Science (UCAS), Beijing, China

¹⁶ Institute of Physics, University of Belgrade, Belgrade, Serbia

¹⁷ Department for Physics and Technology, University of Bergen, Bergen, Norway

¹⁸ Physics Division, Lawrence Berkeley National Laboratory and University of California, Berkeley, CA, United States of America

¹⁹ Institut für Physik, Humboldt Universität zu Berlin, Berlin, Germany

²⁰ Albert Einstein Center for Fundamental Physics and Laboratory for High Energy Physics, University of Bern, Bern, Switzerland

²¹ School of Physics and Astronomy, University of Birmingham, Birmingham, United Kingdom

²² Facultad de Ciencias y Centro de Investigaciones, Universidad Antonio Nariño, Bogotá, Colombia

²³ (a) INFN Bologna and Università di Bologna, Dipartimento di Fisica; (b) INFN Sezione di Bologna, Italy

²⁴ Physikalisches Institut, Universität Bonn, Bonn, Germany

²⁵ Department of Physics, Boston University, Boston, MA, United States of America

²⁶ Department of Physics, Brandeis University, Waltham, MA, United States of America

²⁷ (a) Transilvania University of Brasov, Brasov; (b) Horia Hulubei National Institute of Physics and Nuclear Engineering, Bucharest; (c) Department of Physics, Alexandru Ioan Cuza University of Iasi, Iasi; (d) National Institute for Research and Development of Isotopic and Molecular Technologies, Physics Department, Cluj-Napoca; (e) University Politehnica Bucharest, Bucharest; (f) West University in Timisoara, Timisoara, Romania

²⁸ (a) Faculty of Mathematics, Physics and Informatics, Comenius University, Bratislava; (b) Department of Subnuclear Physics, Institute of Experimental Physics of the Slovak Academy of Sciences, Kosice, Slovak Republic

²⁹ Physics Department, Brookhaven National Laboratory, Upton, NY, United States of America

³⁰ Departamento de Física, Universidad de Buenos Aires, Buenos Aires, Argentina

³¹ California State University, CA, United States of America

³² Cavendish Laboratory, University of Cambridge, Cambridge, United Kingdom

³³ (a) Department of Physics, University of Cape Town, Cape Town; (b) Department of Mechanical Engineering Science, University of Johannesburg, Johannesburg; (c) School of Physics, University of the Witwatersrand, Johannesburg, South Africa

³⁴ Department of Physics, Carleton University, Ottawa, ON, Canada

³⁵ (a) Faculté des Sciences Ain Chock, Réseau Universitaire de Physique des Hautes Energies – Université Hassan II, Casablanca; (b) Faculté des Sciences, Université Ibn-Tofail, Kénitra;

(c) Faculté des Sciences Semlalia, Université Cadi Ayyad, LPHEA, Marrakech; (d) Faculté des Sciences, Université Mohamed Premier and LPTPM, Oujda; (e) Faculté des sciences, Université Mohammed V, Rabat, Morocco

³⁶ CERN, Geneva, Switzerland

³⁷ Enrico Fermi Institute, University of Chicago, Chicago, IL, United States of America

³⁸ LPC, Université Clermont Auvergne, CNRS/IN2P3, Clermont-Ferrand, France

³⁹ Nevis Laboratory, Columbia University, Irvington, NY, United States of America

⁴⁰ Niels Bohr Institute, University of Copenhagen, Copenhagen, Denmark

⁴¹ (a) Dipartimento di Fisica, Università della Calabria, Rende; (b) INFN Gruppo Collegato di Cosenza, Laboratori Nazionali di Frascati, Italy

⁴² Physics Department, Southern Methodist University, Dallas, TX, United States of America

⁴³ Physics Department, University of Texas at Dallas, Richardson, TX, United States of America

⁴⁴ National Centre for Scientific Research "Demokritos", Agia Paraskevi, Greece

⁴⁵ (a) Department of Physics, Stockholm University; (b) Oskar Klein Centre, Stockholm, Sweden

⁴⁶ Deutsches Elektronen-Synchrotron DESY, Hamburg and Zeuthen, Germany

⁴⁷ Lehrstuhl für Experimentelle Physik IV, Technische Universität Dortmund, Dortmund, Germany

⁴⁸ Institut für Kern- und Teilchenphysik, Technische Universität Dresden, Dresden, Germany

⁴⁹ Department of Physics, Duke University, Durham, NC, United States of America

⁵⁰ SUPA – School of Physics and Astronomy, University of Edinburgh, Edinburgh, United Kingdom

⁵¹ INFN e Laboratori Nazionali di Frascati, Frascati, Italy

⁵² Physikalisches Institut, Albert-Ludwigs-Universität Freiburg, Freiburg, Germany

⁵³ II. Physikalisches Institut, Georg-August-Universität Göttingen, Göttingen, Germany

⁵⁴ Département de Physique Nucléaire et Corpusculaire, Université de Genève, Genève, Switzerland

⁵⁵ (a) Dipartimento di Fisica, Università di Genova, Genova; (b) INFN Sezione di Genova, Italy

⁵⁶ II. Physikalisches Institut, Justus-Liebig-Universität Giessen, Giessen, Germany

⁵⁷ SUPA – School of Physics and Astronomy, University of Glasgow, Glasgow, United Kingdom

- ⁵⁸ LPSC, Université Grenoble Alpes, CNRS/IN2P3, Grenoble INP, Grenoble, France
- ⁵⁹ Laboratory for Particle Physics and Cosmology, Harvard University, Cambridge, MA, United States of America
- ⁶⁰ (a) Department of Modern Physics and State Key Laboratory of Particle Detection and Electronics, University of Science and Technology of China, Hefei; (b) Institute of Frontier and Interdisciplinary Science and Key Laboratory of Particle Physics and Particle Irradiation (MOE), Shandong University, Qingdao; (c) School of Physics and Astronomy, Shanghai Jiao Tong University, KLPPAC-MoE, SKLPPC, Shanghai; (d) Tsung-Dao Lee Institute, Shanghai, China
- ⁶¹ (a) Kirchhoff-Institut für Physik, Ruprecht-Karls-Universität Heidelberg, Heidelberg; (b) Physikalisches Institut, Ruprecht-Karls-Universität Heidelberg, Heidelberg, Germany
- ⁶² Faculty of Applied Information Science, Hiroshima Institute of Technology, Hiroshima, Japan
- ⁶³ (a) Department of Physics, Chinese University of Hong Kong, Shatin, N.T., Hong Kong; (b) Department of Physics, University of Hong Kong, Hong Kong; (c) Department of Physics and Institute for Advanced Study, Hong Kong University of Science and Technology, Clear Water Bay, Kowloon, Hong Kong, China
- ⁶⁴ Department of Physics, National Tsing Hua University, Hsinchu, Taiwan
- ⁶⁵ Department of Physics, Indiana University, Bloomington, IN, United States of America
- ⁶⁶ (a) INFN Gruppo Collegato di Udine, Sezione di Trieste, Udine; (b) ICTP, Trieste; (c) Dipartimento Politecnico di Ingegneria e Architettura, Università di Udine, Udine, Italy
- ⁶⁷ (a) INFN Sezione di Lecce; (b) Dipartimento di Matematica e Fisica, Università del Salento, Lecce, Italy
- ⁶⁸ (a) INFN Sezione di Milano; (b) Dipartimento di Fisica, Università di Milano, Milano, Italy
- ⁶⁹ (a) INFN Sezione di Napoli; (b) Dipartimento di Fisica, Università di Napoli, Napoli, Italy
- ⁷⁰ (a) INFN Sezione di Pavia; (b) Dipartimento di Fisica, Università di Pavia, Pavia, Italy
- ⁷¹ (a) INFN Sezione di Pisa; (b) Dipartimento di Fisica E. Fermi, Università di Pisa, Pisa, Italy
- ⁷² (a) INFN Sezione di Roma; (b) Dipartimento di Fisica, Sapienza Università di Roma, Roma, Italy
- ⁷³ (a) INFN Sezione di Roma Tor Vergata; (b) Dipartimento di Fisica, Università di Roma Tor Vergata, Roma, Italy
- ⁷⁴ (a) INFN Sezione di Roma Tre; (b) Dipartimento di Matematica e Fisica, Università Roma Tre, Roma, Italy
- ⁷⁵ (a) INFN-TIFPA; (b) Università degli Studi di Trento, Trento, Italy
- ⁷⁶ Institut für Astro- und Teilchenphysik, Leopold-Franzens-Universität, Innsbruck, Austria
- ⁷⁷ University of Iowa, Iowa City, IA, United States of America
- ⁷⁸ Department of Physics and Astronomy, Iowa State University, Ames, IA, United States of America
- ⁷⁹ Joint Institute for Nuclear Research, Dubna, Russia
- ⁸⁰ (a) Departamento de Engenharia Elétrica, Universidade Federal de Juiz de Fora (UFJF), Juiz de Fora; (b) Universidade Federal do Rio De Janeiro COPPE/EE/IF, Rio de Janeiro; (c) Universidade Federal de São João del Rei (UFSJ), São João del Rei; (d) Instituto de Física, Universidade de São Paulo, São Paulo, Brazil
- ⁸¹ KEK, High Energy Accelerator Research Organization, Tsukuba, Japan
- ⁸² Graduate School of Science, Kobe University, Kobe, Japan
- ⁸³ (a) AGH University of Science and Technology, Faculty of Physics and Applied Computer Science, Krakow; (b) Marian Smoluchowski Institute of Physics, Jagiellonian University, Krakow, Poland
- ⁸⁴ Institute of Nuclear Physics Polish Academy of Sciences, Krakow, Poland
- ⁸⁵ Faculty of Science, Kyoto University, Kyoto, Japan
- ⁸⁶ Kyoto University of Education, Kyoto, Japan
- ⁸⁷ Research Center for Advanced Particle Physics and Department of Physics, Kyushu University, Fukuoka, Japan
- ⁸⁸ Instituto de Física La Plata, Universidad Nacional de La Plata and CONICET, La Plata, Argentina
- ⁸⁹ Physics Department, Lancaster University, Lancaster, United Kingdom
- ⁹⁰ Oliver Lodge Laboratory, University of Liverpool, Liverpool, United Kingdom
- ⁹¹ Department of Experimental Particle Physics, Jožef Stefan Institute and Department of Physics, University of Ljubljana, Ljubljana, Slovenia
- ⁹² School of Physics and Astronomy, Queen Mary University of London, London, United Kingdom
- ⁹³ Department of Physics, Royal Holloway University of London, Egham, United Kingdom
- ⁹⁴ Department of Physics and Astronomy, University College London, London, United Kingdom
- ⁹⁵ Louisiana Tech University, Ruston, LA, United States of America
- ⁹⁶ Fysiska institutionen, Lunds universitet, Lund, Sweden
- ⁹⁷ Centre de Calcul de l'Institut National de Physique Nucléaire et de Physique des Particules (IN2P3), Villeurbanne, France
- ⁹⁸ Departamento de Física Teórica C-15 and CIAFF, Universidad Autónoma de Madrid, Madrid, Spain
- ⁹⁹ Institut für Physik, Universität Mainz, Mainz, Germany
- ¹⁰⁰ School of Physics and Astronomy, University of Manchester, Manchester, United Kingdom
- ¹⁰¹ CPPM, Aix-Marseille Université, CNRS/IN2P3, Marseille, France
- ¹⁰² Department of Physics, University of Massachusetts, Amherst, MA, United States of America
- ¹⁰³ Department of Physics, McGill University, Montreal, QC, Canada
- ¹⁰⁴ School of Physics, University of Melbourne, Victoria, Australia
- ¹⁰⁵ Department of Physics, University of Michigan, Ann Arbor, MI, United States of America
- ¹⁰⁶ Department of Physics and Astronomy, Michigan State University, East Lansing, MI, United States of America
- ¹⁰⁷ B.I. Stepanov Institute of Physics, National Academy of Sciences of Belarus, Minsk, Belarus
- ¹⁰⁸ Research Institute for Nuclear Problems of Byelorussian State University, Minsk, Belarus
- ¹⁰⁹ Group of Particle Physics, University of Montreal, Montreal, QC, Canada
- ¹¹⁰ P.N. Lebedev Physical Institute of the Russian Academy of Sciences, Moscow, Russia
- ¹¹¹ Institute for Theoretical and Experimental Physics of the National Research Centre Kurchatov Institute, Moscow, Russia
- ¹¹² National Research Nuclear University MEPhI, Moscow, Russia
- ¹¹³ D.V. Skobel'syn Institute of Nuclear Physics, M.V. Lomonosov Moscow State University, Moscow, Russia
- ¹¹⁴ Fakultät für Physik, Ludwig-Maximilians-Universität München, München, Germany
- ¹¹⁵ Max-Planck-Institut für Physik (Werner-Heisenberg-Institut), München, Germany
- ¹¹⁶ Nagasaki Institute of Applied Science, Nagasaki, Japan
- ¹¹⁷ Graduate School of Science and Kobayashi-Maskawa Institute, Nagoya University, Nagoya, Japan
- ¹¹⁸ Department of Physics and Astronomy, University of New Mexico, Albuquerque, NM, United States of America
- ¹¹⁹ Institute for Mathematics, Astrophysics and Particle Physics, Radboud University Nijmegen/Nikhef, Nijmegen, Netherlands
- ¹²⁰ Nikhef National Institute for Subatomic Physics and University of Amsterdam, Amsterdam, Netherlands
- ¹²¹ Department of Physics, Northern Illinois University, DeKalb, IL, United States of America
- ¹²² (a) Budker Institute of Nuclear Physics and NSU, SB RAS, Novosibirsk; (b) Novosibirsk State University Novosibirsk, Russia
- ¹²³ Institute for High Energy Physics of the National Research Centre Kurchatov Institute, Protvino, Russia
- ¹²⁴ Department of Physics, New York University, New York, NY, United States of America
- ¹²⁵ Ochanomizu University, Otsuka, Bunkyo-ku, Tokyo, Japan
- ¹²⁶ Ohio State University, Columbus, OH, United States of America
- ¹²⁷ Faculty of Science, Okayama University, Okayama, Japan
- ¹²⁸ Homer L. Dodge Department of Physics and Astronomy, University of Oklahoma, Norman, OK, United States of America
- ¹²⁹ Department of Physics, Oklahoma State University, Stillwater, OK, United States of America
- ¹³⁰ Palacký University, RPTM, Joint Laboratory of Optics, Olomouc, Czech Republic
- ¹³¹ Center for High Energy Physics, University of Oregon, Eugene, OR, United States of America

- ¹³² LAL, Université Paris-Sud, CNRS/IN2P3, Université Paris-Saclay, Orsay, France
- ¹³³ Graduate School of Science, Osaka University, Osaka, Japan
- ¹³⁴ Department of Physics, University of Oslo, Oslo, Norway
- ¹³⁵ Department of Physics, Oxford University, Oxford, United Kingdom
- ¹³⁶ LPNHE, Sorbonne Université, Paris Diderot Sorbonne Paris Cité, CNRS/IN2P3, Paris, France
- ¹³⁷ Department of Physics, University of Pennsylvania, Philadelphia PA, United States of America
- ¹³⁸ Konstantinov Nuclear Physics Institute of National Research Centre "Kurchatov Institute", PNPI, St. Petersburg, Russia
- ¹³⁹ Department of Physics and Astronomy, University of Pittsburgh, Pittsburgh, PA, United States of America
- ¹⁴⁰ ^(a) Laboratório de Instrumentação e Física Experimental de Partículas – LIP; ^(b) Departamento de Física, Faculdade de Ciências, Universidade de Lisboa, Lisboa; ^(c) Departamento de Física, Universidade de Coimbra, Coimbra; ^(d) Centro de Física Nuclear da Universidade de Lisboa, Lisboa; ^(e) Departamento de Física, Universidade do Minho, Braga; ^(f) Universidad de Granada, Granada (Spain); ^(g) Dep Física and CEFITEC of Faculdade de Ciências e Tecnologia, Universidade Nova de Lisboa, Caparica, Portugal
- ¹⁴¹ Institute of Physics of the Czech Academy of Sciences, Prague, Czech Republic
- ¹⁴² Czech Technical University in Prague, Prague, Czech Republic
- ¹⁴³ Charles University, Faculty of Mathematics and Physics, Prague, Czech Republic
- ¹⁴⁴ Particle Physics Department, Rutherford Appleton Laboratory, Didcot, United Kingdom
- ¹⁴⁵ IRFU, CEA, Université Paris-Saclay, Gif-sur-Yvette, France
- ¹⁴⁶ Santa Cruz Institute for Particle Physics, University of California Santa Cruz, Santa Cruz, CA, United States of America
- ¹⁴⁷ ^(a) Departamento de Física, Pontificia Universidad Católica de Chile, Santiago; ^(b) Departamento de Física, Universidad Técnica Federico Santa María, Valparaíso, Chile
- ¹⁴⁸ Department of Physics, University of Washington, Seattle, WA, United States of America
- ¹⁴⁹ Department of Physics and Astronomy, University of Sheffield, Sheffield, United Kingdom
- ¹⁵⁰ Department of Physics, Shinshu University, Nagano, Japan
- ¹⁵¹ Department Physik, Universität Siegen, Siegen, Germany
- ¹⁵² Department of Physics, Simon Fraser University, Burnaby, BC, Canada
- ¹⁵³ SLAC National Accelerator Laboratory, Stanford, CA, United States of America
- ¹⁵⁴ Physics Department, Royal Institute of Technology, Stockholm, Sweden
- ¹⁵⁵ Departments of Physics and Astronomy, Stony Brook University, Stony Brook, NY, United States of America
- ¹⁵⁶ Department of Physics and Astronomy, University of Sussex, Brighton, United Kingdom
- ¹⁵⁷ School of Physics, University of Sydney, Sydney, Australia
- ¹⁵⁸ Institute of Physics, Academia Sinica, Taipei, Taiwan
- ¹⁵⁹ ^(a) E. Andronikashvili Institute of Physics, Iv. Javakishvili Tbilisi State University, Tbilisi; ^(b) High Energy Physics Institute, Tbilisi State University, Tbilisi, Georgia
- ¹⁶⁰ Department of Physics, Technion, Israel Institute of Technology, Haifa, Israel
- ¹⁶¹ Raymond and Beverly Sackler School of Physics and Astronomy, Tel Aviv University, Tel Aviv, Israel
- ¹⁶² Department of Physics, Aristotle University of Thessaloniki, Thessaloniki, Greece
- ¹⁶³ International Center for Elementary Particle Physics and Department of Physics, University of Tokyo, Tokyo, Japan
- ¹⁶⁴ Graduate School of Science and Technology, Tokyo Metropolitan University, Tokyo, Japan
- ¹⁶⁵ Department of Physics, Tokyo Institute of Technology, Tokyo, Japan
- ¹⁶⁶ Tomsk State University, Tomsk, Russia
- ¹⁶⁷ Department of Physics, University of Toronto, Toronto, ON, Canada
- ¹⁶⁸ ^(a) TRIUMF, Vancouver, BC; ^(b) Department of Physics and Astronomy, York University, Toronto, ON, Canada
- ¹⁶⁹ Division of Physics and Tomonaga Center for the History of the Universe, Faculty of Pure and Applied Sciences, University of Tsukuba, Tsukuba, Japan
- ¹⁷⁰ Department of Physics and Astronomy, Tufts University, Medford, MA, United States of America
- ¹⁷¹ Department of Physics and Astronomy, University of California Irvine, Irvine, CA, United States of America
- ¹⁷² Department of Physics and Astronomy, University of Uppsala, Uppsala, Sweden
- ¹⁷³ Department of Physics, University of Illinois, Urbana, IL, United States of America
- ¹⁷⁴ Instituto de Física Corpuscular (IFIC), Centro Mixto Universidad de Valencia – CSIC, Valencia, Spain
- ¹⁷⁵ Department of Physics, University of British Columbia, Vancouver, BC, Canada
- ¹⁷⁶ Department of Physics and Astronomy, University of Victoria, Victoria, BC, Canada
- ¹⁷⁷ Fakultät für Physik und Astronomie, Julius-Maximilians-Universität Würzburg, Würzburg, Germany
- ¹⁷⁸ Department of Physics, University of Warwick, Coventry, United Kingdom
- ¹⁷⁹ Waseda University, Tokyo, Japan
- ¹⁸⁰ Department of Particle Physics, Weizmann Institute of Science, Rehovot, Israel
- ¹⁸¹ Department of Physics, University of Wisconsin, Madison, WI, United States of America
- ¹⁸² Fakultät für Mathematik und Naturwissenschaften, Fachgruppe Physik, Bergische Universität Wuppertal, Wuppertal, Germany
- ¹⁸³ Department of Physics, Yale University, New Haven, CT, United States of America
- ¹⁸⁴ Yerevan Physics Institute, Yerevan, Armenia

^a Also at Centre for High Performance Computing, CSIR Campus, Rosebank, Cape Town, South Africa.

^b Also at CERN, Geneva, Switzerland.

^c Also at CPPM, Aix-Marseille Université, CNRS/IN2P3, Marseille, France.

^d Also at Département de Physique Nucléaire et Corpusculaire, Université de Genève, Genève, Switzerland.

^e Also at Departament de Física de la Universitat Autònoma de Barcelona, Barcelona, Spain.

^f Also at Departamento de Física, Instituto Superior Técnico, Universidade de Lisboa, Lisboa, Portugal.

^g Also at Department of Applied Physics and Astronomy, University of Sharjah, Sharjah, United Arab Emirates.

^h Also at Department of Financial and Management Engineering, University of the Aegean, Chios, Greece.

ⁱ Also at Department of Physics and Astronomy, University of Louisville, Louisville, KY, United States of America.

^j Also at Department of Physics and Astronomy, University of Sheffield, Sheffield, United Kingdom.

^k Also at Department of Physics, California State University, East Bay, United States of America.

^l Also at Department of Physics, California State University, Fresno, United States of America.

^m Also at Department of Physics, California State University, Sacramento, United States of America.

ⁿ Also at Department of Physics, King's College London, London, United Kingdom.

^o Also at Department of Physics, St. Petersburg State Polytechnical University, St. Petersburg, Russia.

^p Also at Department of Physics, Stanford University, Stanford CA, United States of America.

^q Also at Department of Physics, University of Fribourg, Fribourg, Switzerland.

^r Also at Department of Physics, University of Michigan, Ann Arbor MI, United States of America.

^s Also at Faculty of Physics, M.V. Lomonosov Moscow State University, Moscow, Russia.

^t Also at Giresun University, Faculty of Engineering, Giresun, Turkey.

^u Also at Graduate School of Science, Osaka University, Osaka, Japan.

- ^v Also at Hellenic Open University, Patras, Greece.
- ^w Also at Institutio Catalana de Recerca i Estudis Avancats, ICREA, Barcelona, Spain.
- ^x Also at Institut für Experimentalphysik, Universität Hamburg, Hamburg, Germany.
- ^y Also at Institute for Mathematics, Astrophysics and Particle Physics, Radboud University Nijmegen/Nikhef, Nijmegen, Netherlands.
- ^z Also at Institute for Nuclear Research and Nuclear Energy (INRNE) of the Bulgarian Academy of Sciences, Sofia, Bulgaria.
- ^{aa} Also at Institute for Particle and Nuclear Physics, Wigner Research Centre for Physics, Budapest, Hungary.
- ^{ab} Also at Institute of High Energy Physics, Chinese Academy of Sciences, Beijing, China.
- ^{ac} Also at Institute of Particle Physics (IPP), Canada.
- ^{ad} Also at Institute of Physics, Academia Sinica, Taipei, Taiwan.
- ^{ae} Also at Institute of Physics, Azerbaijan Academy of Sciences, Baku, Azerbaijan.
- ^{af} Also at Institute of Theoretical Physics, Ilia State University, Tbilisi, Georgia.
- ^{ag} Also at Instituto de Fisica Teorica, IFT-UAM/CSIC, Madrid, Spain.
- ^{ah} Also at Istanbul University, Dept. of Physics, Istanbul, Turkey.
- ^{ai} Also at Joint Institute for Nuclear Research, Dubna, Russia.
- ^{aj} Also at LAL, Université Paris-Sud, CNRS/IN2P3, Université Paris-Saclay, Orsay, France.
- ^{ak} Also at Louisiana Tech University, Ruston LA, United States of America.
- ^{al} Also at LPNHE, Sorbonne Université, Paris Diderot Sorbonne Paris Cité, CNRS/IN2P3, Paris, France.
- ^{am} Also at Manhattan College, New York NY, United States of America.
- ^{an} Also at Moscow Institute of Physics and Technology State University, Dolgoprudny, Russia.
- ^{ao} Also at National Research Nuclear University MEPhI, Moscow, Russia.
- ^{ap} Also at Physics Department, An-Najah National University, Nablus, Palestine.
- ^{aq} Also at Physics Dept, University of South Africa, Pretoria, South Africa.
- ^{ar} Also at Physikalisches Institut, Albert-Ludwigs-Universität Freiburg, Freiburg, Germany.
- ^{as} Also at School of Physics, Sun Yat-sen University, Guangzhou, China.
- ^{at} Also at The City College of New York, New York NY, United States of America.
- ^{au} Also at The Collaborative Innovation Center of Quantum Matter (CICQM), Beijing, China.
- ^{av} Also at Tomsk State University, Tomsk, and Moscow Institute of Physics and Technology State University, Dolgoprudny, Russia.
- ^{aw} Also at TRIUMF, Vancouver BC, Canada.
- ^{ax} Also at Università di Napoli Parthenope, Napoli, Italy.
- * Deceased.